

# **Qulleq-1 (6354/4-1): petrography of selected sidewall cores**

Service report prepared for Statoil a.s

Thomas Preuss and Finn Dalhoff



# **Qulleq-1 (6354/4-1): petrography of selected sidewall cores**

Service report prepared for Statoil a.s

Thomas Preuss and Finn Dalhoff

Released 01.04.2001

# Contents

<b>Summary</b>	<b>3</b>
<b>Introduction</b>	<b>3</b>
<b>Detrital mineralogy and textures</b>	<b>4</b>
Sandstone classification .....	4
Quartz.....	5
Feldspar .....	6
Mica .....	6
Rock fragments.....	6
Glauconite .....	6
Heavy minerals .....	6
Organic material.....	6
Bioclasts.....	6
<b>Mechanical compaction</b>	<b>7</b>
<b>Authigenic mineralogy</b>	<b>7</b>
Kaolinite .....	7
Ti-oxide .....	7
Chlorite.....	7
Pyrite .....	7
Siderite .....	8
Goethite.....	8
Illite .....	8
Feldspar .....	8
Quartz.....	8
Calcite .....	9
K-minerals .....	9
<b>Porosity</b>	<b>9</b>
Total porosity.....	9
Primary porosity .....	9
Secondary porosity .....	10
Permeability .....	10
<b>Provenance</b>	<b>10</b>
<b>Diagenesis</b>	<b>11</b>
<b>Conclusion</b>	<b>12</b>
<b>References</b>	<b>14</b>
<b>Figures 1–4</b>	
<b>Table 1</b>	
<b>Plates 1–23</b>	

## Summary

The present report summarises the petrographic description of thirteen sidewall cores from Statoils well 6354/4-1 (Qulleq-1), drilled offshore West Greenland in the summer 2000.

Qulleq-1 was situated at:

Latitude: 63°48'48.03"N

Longitude: 54°27'06.61"W

in the Fylla licence area (Fig. 1) at a water depth of 1152 m. The well was spudded on 10 July, 2000 and reached TD of 2973 m below RT on 4 September 2000 in Upper Santonian? sandstones. Qulleq-1 was plugged and abandoned as a dry hole on 3 October 2000.

## Introduction

Petrographic analyses have been carried out on selected sidewall cores from Qulleq-1 in order to investigate the diagenetic history and possible provenance of the sandstones.

Thirteen sidewall core samples were selected, and impregnated by blue epoxy prior to thin section preparation. The thin sections were polished, and no staining methods were used. The unconsolidated nature of the samples made the preparation of the thin sections difficult and resulted in a thickness over the preferred 30 µm. The consequence of this is too high interference colours of the minerals making identification more difficult. Counting of 300 points were carried out for 9 of the thin sections, the last four being so fragmented due to preparation, that this number could not be achieved. The polished thin sections were carbon-coated, before examined by scanning electron microscopy (SEM) on a Philips XL40 SEM, revealing secondary electron (SE)- and backscattered electron (BSE) imaging. X-ray element mapping was performed on the SEM with a Noran Vantage Energy Dispersive Spectral (EDS) system. The SEM was equipped with a tungsten filament for analysis.

The selected sample descriptions, taken from Preuss *et al.* 2000, are listed below with all depths referred to the RT, as reported by Statoil:

- 23 (Run 2B) 2655m Sst, fs-ms, light w. green spots, loose, qu, glau., mica, dark min., well-sort., round-subround.
- 22 (Run 2B) 2662m Sst, ms-cs, grey w. green spots, loose, qu, glau., dark min., well-sort., round-subround, calcareous.

- 17 (Run 2C) 2671m Sst, fs-ms, grey-green, loose, qu, glau., dark min., mica, well-sort., round.-subround., calcareous.
- 21 (Run 2B) 2676m Sst, fs-ms, grey-green, loose, qu, glau., dark. min., well-sort., ang.-subround., calcareous.
- 16 (Run 2C) 2682m Sst, fs-ms, light-grey w. dark streaks, loose, qu, glau., dark min., mudst. clasts, Fe-ox, well-sort., calcareous.
- 20 (Run 2B) 2686m Sst, vf-ms w. dark silt streaks, loose, grey, qu, mica, dark min., well-sort. sst, calcareous.
- 15 (Run 2C) 2696m Sst, vfs-fs, grey w. dark streaks, loose, qu, mica, dark min., well-sort., subround. calcareous.
- 16 (Run 2B) 2738m Silty sst, silt-fs with mudstreaks, grey-green, loose, qu, mica, dark min., pyrite, poorly sort., sub-round., non-calcareous.
- 15 (Run 2B) 2755m Sst, vf-ms, grey-green, loose, qu, mica, dark min., mod. sort., ang.-subang., calcareous.
- 9 (Run 2C) 2853m Sst with granules (<1 cm), fs-cs, grey-green, loose, qu, ?glau., poorly sort., calcareous.
- 7 (Run 2C) 2885m Sst w. granules, fs-cs, grey-green, loose, qu, glau., dark min., poorly sort., subround., calcareous.
- 3 (Run 2C) 2894m Sst, fs, light green, loose, qu, few dark and red min., well-sort., calcareous.
- 6 (Run 2B) 2906.5m Sst, vf, greenish, loose, qu., mica, well-sort., round.-subround., non-calcareous.

It must be emphasised that the original texture was largely destroyed during sampling of the sidewall cores due to the unconsolidated nature of the sandstones. The detrital minerals have also suffered intense crushing due to the sampling technique.

## **Detrital mineralogy and textures**

Point counting data can be found in Table 1.

**Sandstone classification.** The sandstones are classified as arkoses and lithic arkoses following Folk (1968), see Fig. 2. The samples are immature with a high content of feldspar. The highest contents of rock fragments are found in the coarsest samples. An attempt to classify the sandstone before diagenetic influence is shown on Fig. 3. Point counting values mainly from kaolinite replacement and secondary porosity in feldspars are reversed to restore the original composition of the sandstones. The change in sandstone classification

reflecting the diagenetic pathway is illustrated on Fig. 4. The classification does not change that much for each sample although the dissolution of feldspar grains lead to a more quartz- and lithic composition. The sandstone classification of the samples is relatively uniform suggesting sediment supply from the same source area during deposition.

Grain-sizes vary from very fine- to coarse-grained, locally pebbly, and grain sorting varies from very well to poorly sorted. The overall tendency for grain-size and -sorting is that the most fine-grained samples are well to very well-sorted, whereas the most coarse-grained samples are poorly sorted. Medium-grained samples tend to be moderately sorted. Grain form is dominantly subangular, although certain grain types, like glauconite, zircons, large rock fragments and a minor part of the quartz, are well rounded. The rock fragments in the sandstones are dominated by slightly metamorphosed, plutonic rock, except from the deepest of the point counted samples (2894m) where metamorphic rocks dominate. However, there are so few rock fragments in the sample that it is uncertain to conclude whether it marks a shift in provenance.

A few samples contain up to 7.0% of detrital matrix composed of a mixture of small, grain particles in intergranular pore-space. The feldspar fragments are often partly dissolved, and it can not be excluded that the matrix in some instances represents the remnants of intensively dissolved detrital grains or rock fragments.

The high feldspar content and the content of ferromagnesian grains, although diagenetically altered, define the sand as immature and indicates deposition with little reworking. The sub-angularity of the grains and the moderate to poor sorting of the medium to coarse-grained samples point to a proximal depositional area for the sand, which did not experience long transportation.

The main provenance area is believed to have been plutonic with a metamorphic overprint. Rounded quartz grains indicate a minor contribution from reworked sediments, and the content of well-rounded glauconite grains strongly indicates reworking of marine sediments deposited at low water-depths.

**Quartz** (modal range 18.3–49.7%) is the dominant detrital phase, comprising predominantly un- to slightly strained monocrystalline grains. The degree of extinction varies from dominantly straight to strongly undulose. The main part of the quartz grains is subangular, but rounded grains do occur and could represent a recycled, sedimentary source.

**Feldspar** (modal range 11.3–18.0%) grains are dominated by **plagioclase** (modal range 7.3–14.7%), although **kalifeldspar** (modal range 1.3–5.0%) are present in all samples. The plagioclase grains are dominantly Na-rich with a minor calcium content. The kalifeldspar grains are identified as microcline. The feldspars often show signs of dissolution or replacement by other diagenetic phases like kaolinite and calcite. Furthermore feldspars are the main target for secondary porosity in the sandstones, and 47.6–78.1% with an average of 59.7% of the point-counted plagioclase, and 9.1–60.0% with an average of 25.2% of the kalifeldspar are partly dissolved. This indicates a diagenetic environment less stable for plagioclase compared to kalifeldspar.

The **mica** content (modal range 1.3–29.7%) is highest in the fine-grained samples, and with greenish **biotite** as the major and **muscovite** as the minor phase. The most fine-grained sample (2686m) shows the highest concentration (29.7%), see Plate 10, 11 and 12.

**Rock fragments** (modal range 1.7–7.3%) comprises a minor range of slightly metamorphosed, plutonic grains as the dominant type and some metamorphic clasts, while sedimentary grains are represented by a few illitic mudstone clasts and chert grains. Large, rock fragments are very well rounded.

**Glaucinite** grains (modal range 0–8.0%) are dark green, well to very well rounded, and they often reveal cracks, see Plate 1, 2, 4, 5, 14 and 15. Some of the grains are deformed due to compaction, see Plate 6 and 7. The glauconite content is highest in the samples above 2682m. The glauconite grains was formed in a marine environment and probably transported before deposition.

**Heavy minerals** (modal range trace–0.3%) represent rounded zircon grains detected in all samples.

**Organic material** (modal range 0.3–5.3%) is found in all samples. It is mechanical compacted, coalified and often accompanied by authigene pyrite, see Plate 13. The organic material often makes up laminae in the samples, see Plate 10, 11 and 12.

**Bioclasts** are not found in the thin sections, although foraminifera have been recorded in cores from mudstones at lower depth.

## Mechanical compaction

Point-contacts are the dominant contact type between detrital grains in the samples. The original fracture pattern in the sediment is difficult to recognise due to the intense fracturing related to the sampling technique of the sidewall cores. Although the main part of the fractures and grain cracks are believed to reflect sampling, some grain cracks are filled with cement types, and thus pre-date these authigene phases, see Plate 1, 2, 3, 4, 5, 6 and 7. Mechanical compaction resulted in cracks of detrital grains at point contacts and bending of mica and organic material. Mica is bent around detrital feldspar grains that have suffered later dissolution or replacement by kaolinite, see Plate 8 and 9. Siderite precipitation along cleavage planes in mica grains follow the outline of the deformed grain thus post dating mechanical compaction, see Plate 10, 11 and 12. The first authigene mineral phase, kaolinite is found in grain cracks, and thus mechanical compaction is considered the earliest event in the sandstones. Only a few tangential contacts between detrital quartz and mica grains are observed, indicating that pressure dissolution was only of minor importance in the sandstones, see Plate 13.

## Authigenic mineralogy

The main authigenic phases present are kaolinite, Ti-oxide, quartz and calcite cement, with minor pyrite, goethite, illite, feldspar and chlorite also recognised. The authigenic minerals are listed in order of diagenetic appearance.

**Kaolinite** (modal range 3.7–15.0%) is recognised in all samples, with the highest value found in the shallowest sample (2655m). It mainly occurs in or adjacent to feldspar dissolution voids, see Plate 16 and 17, as well as in oversize pore space where it occur as booklets, see Plate 1, 2, 4, 5, 18 and 19. Grain remnants indicate that both plagioclase and kalifeldspar grains have suffered replacement. Some kaolinitisation of mica also occurred.

**Ti-oxide** (modal range 0.3–5.3%) is localised near dissolved ferromagnesian grains predominantly biotite, where it often is precipitated between cleavage planes.

**Chlorite** (modal range trace–3.7%) is precipitated as flakes, often near Ti-oxides that replace ferromagnesian grains.

**Pyrite** (modal range trace–5.0%) is found as replacement of unstable, iron-rich, detrital grains, or, dominantly, in close connection with organic debris. The

samples with the highest concentration of organic debris reveal the highest concentration of pyrite and bands of pyrite often follows fine-grained laminas in the samples. One pyrite crystal with a diameter of 1 cm is found in sample 2738m. Pyrite is seen to have precipitated in cracks of detrital grains, see Plate 3, and thus post dating mechanical compaction. Pyrite is also seen to engulf early kaolinite booklets.

**Siderite** (modal range 0–9.3%) is observed in four samples (2671m, 2676m, 2686m and 2696m), with the highest concentration in sample 2686m, the only one with a content above trace amount. The siderite crystals form flattened rhombs, precipitated along cleavage planes in mica grains and as smaller crystals in mudstone clasts, see Plate 10, 11 and 12. Siderite precipitation has often expanded the mica flakes. EDS-analysis reveals relatively high amounts of Mn, Mg and Ca compared to Fe in the siderites, thus indicating a marine, diagenetic environment.

**Goethite** (modal range 0–1.7%) is only found in sample 2885m. It is characterised by yellowish, euhedral crystals around 40 µm, an orthorhombic form sometimes revealing a hexagonal outline in transverse section, see Plate 20. It is precipitated along cleavage plains in biotite grains, where the flakes have expanded considerably. The goethite is often located in small, rhombic, intra-granular pore spaces, which it occasionally fails to fill out, see Plate 21. The crystals also occur concentrated in pore spaces near intensely degraded biotite grains, see Plate 20. EDS-analysis reveals, that the crystals are rich in iron with a minor content of Mn and Si. The goethite is believed to have replaced siderite rhombs precipitated at an early stage reflected by the considerably expansion. The transformation explains the rhombic form of the goethite crystals, revealing the former siderite morphology sometimes only preserved as rhombic cavities in the biotite. The goethite crystals often show signs of dissolution.

**Illite** (modal range 0–2.0%) occurs with a flaky morphology near partly to complete dissolved feldspar grains and scattered in the matrix.

**Feldspar** (modal range trace amount) overgrowth is only observed in one of the deepest samples 2894m. The overgrowth is situated on a kaolinite-replaced grain, and it follows the outline of a compacted mudstone clast thus post dating mechanical compaction, see Plate 22 and 23. Small, euhedral crystals, believed to represent authigene feldspars, are overgrown by quartz.

**Quartz** (modal range 1.3–4.3%) occurs as overgrowths on detrital grains. The overgrowths are usually small, and no pore-closing authigene quartz has been

observed. Secondary porosity after feldspar dissolution in rock fragments is partly reduced by quartz ingrowths before calcite cementation, see Plate 1, 2, 6 and 7. Authigene quartz engulfs kaolinite, pyrite and siderite, thus post-dating these phases. There seems to be a tendency for enhanced quartz overgrowths in the well-sorted, fine-grained samples.

**Calcite** (modal range 0–13.0 %) reveals a high concentration in one sample (2662m), while the others have an amount between 0 and 2.0%. It has a patchy occurrence dominantly as poikilotopic crystals, which fill up pore space and make up intergranular cement. Calcite is also seen to replace detrital feldspar grains also as a part of rock fragments, see Plate 1 and 2. Calcite occurs in cracks of crushed feldspar and glauconite grains, where it is unaffected by later feldspar dissolution, see Plate 4, 5, 14, 15, 6 and 7. This late feldspar dissolution which resulted in secondary porosity, does not seem to have affected the surrounding calcite cement, see Plate 14 and 15. Since quartz overgrowths are cemented by calcite, it is believed that the authigene quartz phase stopped at the time of calcite precipitation, see Plate 6 and 7.

**K-minerals** are summed in Table 1. The purpose is to compare the content of K-minerals in the samples with the peaks observed on the log pattern. No obvious correlation is found, but it is believed that the log pattern responds to the higher content of biotite in the fine-grained samples.

## **Porosity**

Porosity values obtained by point counting can be found in Table 1.

**Total porosity** values varies between 4.3 and 15.3% with an average of 9.8%. The sample with the lowest porosity value is the most fine-grained one. No correlation between porosity values and depth is observed.

The total porosity numbers are significantly lower than the original number in the undisturbed sediment due to a compaction effect from core sampling. Furthermore, the loose state of the sidewall cores made the preparation process difficult; thus many of the thin sections are twice the normal thickness of 30 µm. The enhanced thickness makes mineral identification more difficult, like it will tend to underestimate porosity values by point-counting, primary as well as secondary.

**Primary porosity** (modal range 0.3–2.0%) makes up a very low number of the

total porosity. This low number would normally reflect a well-cemented rather than a loose-cemented sandstone. The main reason for the low values of primary porosity is compaction and intense grain crushing due to the sampling of the loose sandstones, which makes it difficult to estimate the original primary porosity.

**Secondary porosity** (modal range 4.0–13.7%) accounts for 74.0–96.1% of the total amount of porosity. It is mainly due to dissolution of detrital feldspar, which accounts for 35.1–73.0%, with an average of 59.7%, of the total secondary porosity. Secondary porosity in feldspars is mainly due to plagioclase dissolution, with values of 72.6–100% compared to kalifeldspar dissolution.

The first development of secondary porosity was due to feldspar dissolution, but precipitation of kaolinite reduced the gain in porosity considerably. The loose texture of the kaolinite booklets reveals around 40% of microporosity. If this is included, the total porosity number of the samples will be enhanced to a total of 6.3–18.3%.

The second and most important development of secondary porosity due to feldspar dissolution is also the latest and probably still active diagenetic phase in the sediment.

**Permeability.** The moderate to poor sorting of the medium- to coarse-grained sandstones results in a lower permeability due to blocking of the pore throats by small, detrital components. The same problem is reflected by the content of kaolinite, well known to be a problem in production by its pore blocking effect. Illite flakes and laths have a destructive effect on permeability, and thus the low illite content in the sandstones is considered an advantage.

## **Provenance**

The relatively immature texture and composition of the sediment reflect a limited transportation of the sand deposited rather proximal to the source area. This area was characterised by slightly metamorphic, plutonic rocks. Rounded grains reflect a minor input from eroded sediments. Higher concentrations of well-rounded glauconite grains above 2682m in the upper part of the sedimentary sequence indicate redeposition of marine sediments deposited at low water depths. The erosive episode could reflect a tectonic event or changes in sea level.

## Diagenesis

After deposition, compaction was initiated. Bending of mica grains and crushing of some feldspar and glauconite grains at point contacts, may suggest heavy overburden before mechanical rearrangement of the grain texture distributed stress contacts. This could be evidence of a high sedimentation rate for the deposited sand at Qulleq-1.

After initial deposition and mechanical compaction of the sandstone, the first diagenetic event appears to have been kaolinite precipitation. Aggressive pore waters, most likely in form of penetrating meteoric water or as a result of degrading organic matter in the sediment, lead to dissolution of detrital grains. It was mainly feldspars, that were partly to completely transformed into kaolinite. Thus the increase in secondary porosity at this early stage was mainly due to microporosity between the loosely packed kaolinite booklets. The dissolution of feldspars increased the concentration of silica in the pore water.

The reducing environment established in connection with degrading organic matter favoured pyrite precipitation. The degradation transferred sulphate into sulphide, which reacted with reduced iron to form pyrite. The sulphate needed for the diagenetic reaction indicates a marine environment.

Rhombic siderite is closely connected to biotite grains and mudstone clasts, maybe as a consequence of a local, alkaline microenvironment between the flakes or in the low porous mudstone clasts. The chemical composition of the siderites indicates a marine diagenetic environment.

Siderite crystals were transformed into goethite crystals in one of the deepest samples (2885m). The transformation from siderite to goethite needs oxidising water, and this could reflect that the sediments, at least at this depth, experienced a renewed flux of oxidising meteoric water, maybe as a result of uplift. Another explanation is that the meteoric water front causing kaolinite precipitation first arrived at this depth after siderite precipitation.

Dissolution of ferro-titanium minerals in the immature sediment resulted in precipitation of Ti-oxides. The low solubility of Ti concentrated the Ti-oxides in the vicinity of the original grain, while at least some of the dissolved iron was reprecipitated as chlorite near the Ti-oxides.

The few observed feldspar overgrowths probably reflect local supersaturating due to feldspar dissolution.

Quartz overgrowth was most likely an ongoing process, and since there is only a few signs of pressure dissolution between quartz and mica grains, it is believed that dissolved and replaced feldspar grains have supplied the silica needed for the process.

Calcite precipitation indicates an alkaline diagenetic environment with pore water saturated with calcium. The calcium was most likely supplied from the dissolved and replaced feldspars, but the high variance in the calcite content between samples with the same feldspar content indicates an additional source of calcium at some levels. This additional source could be biogenic grains, which after dissolution acted as the main calcium source at certain levels in the marine sediment. The intergranular calcite cement is totally pore space occluding, but due to its patchy occurrence it is not believed to have formed significant vertical permeability barriers. Thus an open pore system was maintained, allowing fluid circulation to continue. The patchy calcite cement helped stabilising the loosely cemented sediment.

Renewed feldspar dissolution with formation of secondary porosity followed calcite precipitation. The new aggressive pore waters, which percolated the sediments, were most likely expelled as compaction waters from surrounding organic-rich mudstones. Though the dissolution process did not seem to affect the surrounding calcite, the possibility that some calcite dissolution occurred at this last diagenetic stage cannot be ruled out.

## **Conclusion**

Immature arkosic sand was deposited in a marine environment proximal to a slightly metamorphosed, plutonic source area. Rounded quartz and glauconite grains indicate a minor input from sedimentary sources, especially above 2682m in the upper part of the sedimentary sequence.

Following mechanical compaction with some grain crushing, incipient kaolinite replacement of detrital feldspar grains resulted in microporosity. This is believed to reflect a flux of topographic driven aggressive, meteoric water from the hinterland into the marine sediments.

Siderite precipitation was restricted to certain levels and microenvironments, like mica grains and mudstone clasts, with enhanced alkalinity. In a sample from the deeper level (2885m), the siderite is replaced by goethite due to an

oxidising event. This could either reflect a renewed flux of meteoric water due to uplift or a depth-related delay in the meteoric waterfront responsible for kaolinite precipitation, but post-dating siderite precipitation in the deeper parts of the sediments.

Quartz overgrowths were widespread, but of minor volumetric importance, and without a pore-closing feature. The ongoing feldspar dissolution process is believed to have supplied the silica.

Intergranular calcite precipitation reduced primary and secondary porosity, but its patchy occurrence seems to exclude the formation of effective diagenetic barriers, which could have reduced pore-water circulation. Feldspars and biogenic grains are believed to have supplied the calcium needed.

The latest and probably still active process in the sediments is the second generation of secondary porosity. Detrital feldspar grains are dissolved by aggressive percolating pore-water, leaving the surrounding calcite unaffected. The pore water probably represents acid water expelled from surrounding organic-rich mudstones by compaction.

No relation between depth and porosity- and permeability values has been found in the sandstones.

No relation between the total concentration of K-minerals and the log peaks has been found. The peaks are believed to reflect higher concentrations of biotite in fine-grained intervals.

## References

Folk, R.L., 1968, Petrology of sedimentary rocks. Austin, Texas, Hemphill's Book Store, 170 pp.

Preuss, T., Dam, G. and Dalhoff, F. 2001. Qulleq-1 (6354/4-1): sidewall core description. Service report prepared for Statoil a.s., Danmarks og Grønland Geologiske Undersøgelse Rapport **2001/4**, 31 pp.

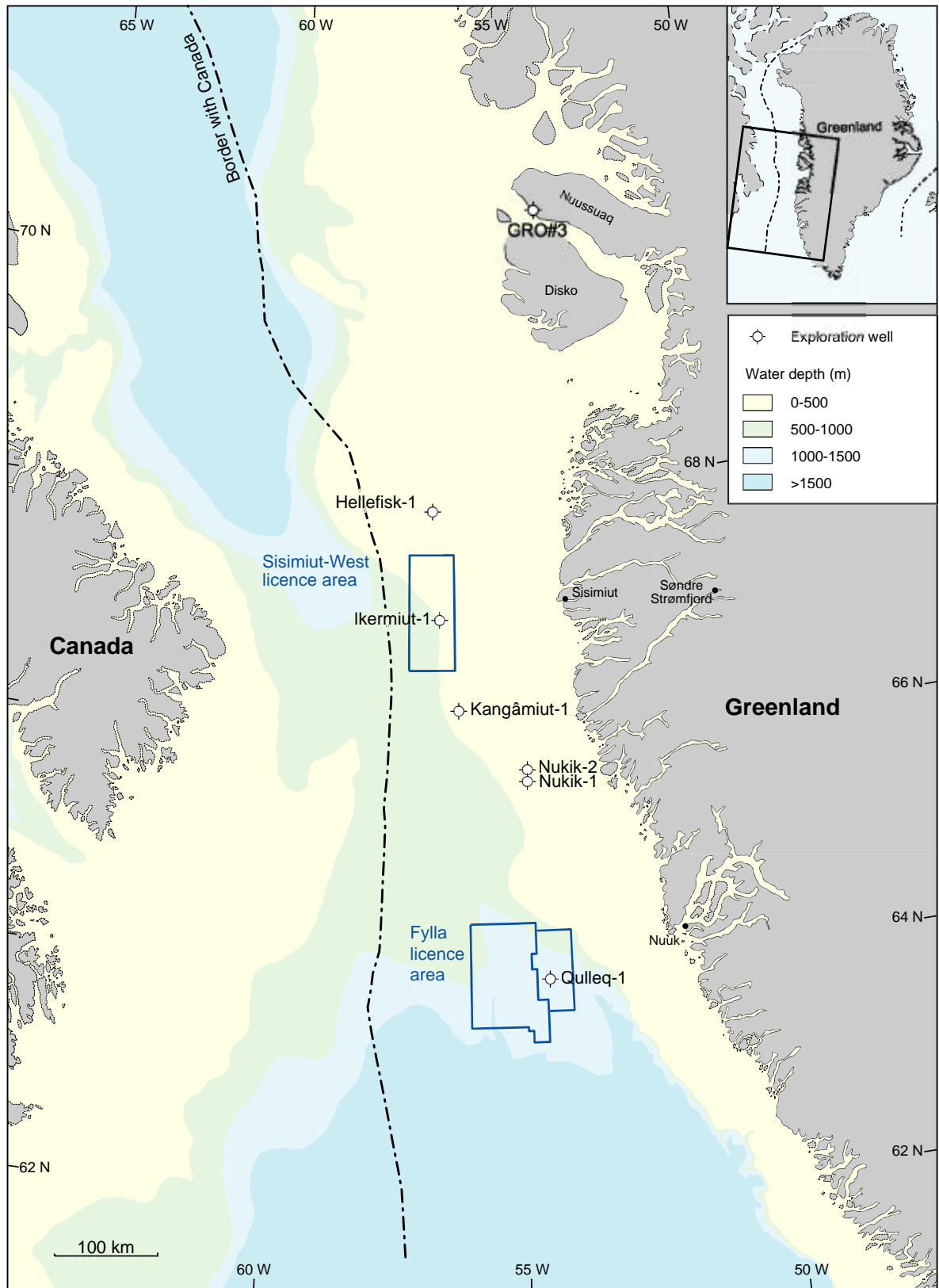


Figure 1. Location map.

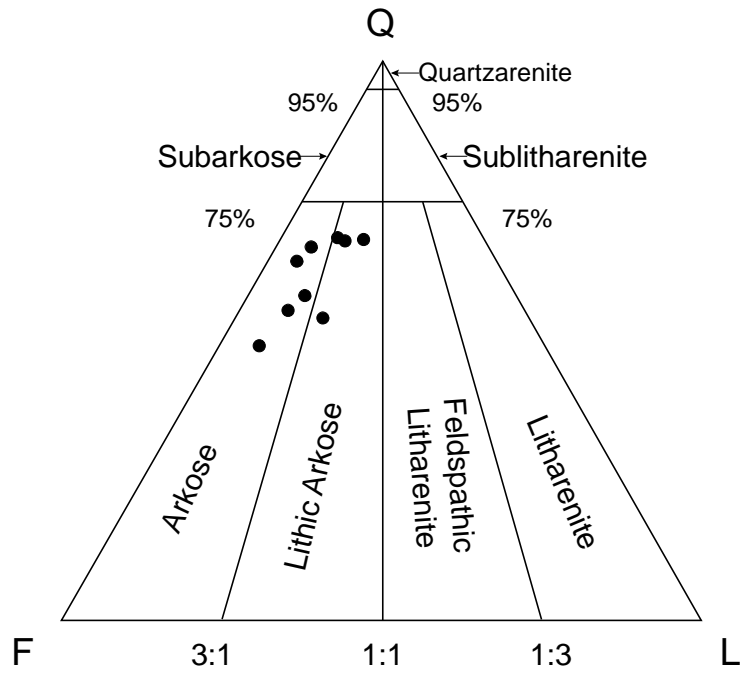


Figure 2. Point counting data in percent from selected thin sections from Qulleq-1, where an amount of 300 points could be obtained. Sandstone classification according to Folk (1968).

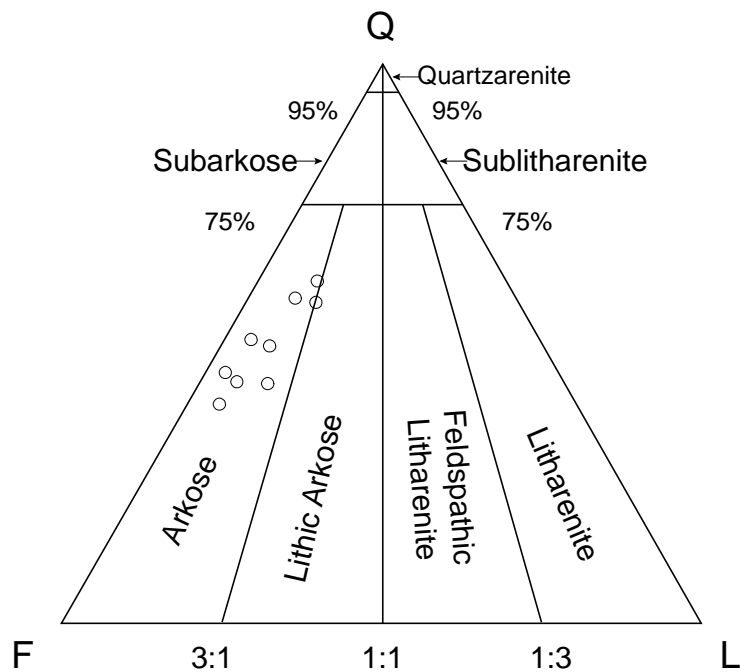


Figure 3. Sandstone classification according to Folk (1968) after attempt has been made to calculate the original composition of the sandstone before diagenetic changes, mainly affecting feldspars.

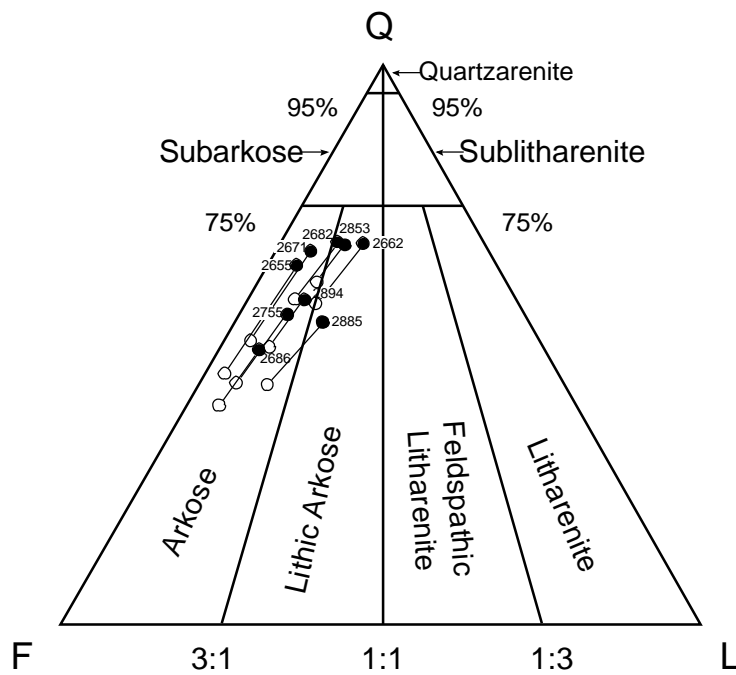


Figure 4. The diagenetic trend of the point-counted sandstones from Qulleq-1 reflected by sandstone classification (Folk, 1968). The enrichment in quartz content relative to feldspar is obvious. Numbers refer to depth, filled and open dots are data from Figure 2 and 3 respectively.

Depth	2655m	2662m	2671m	2682m	2686m	2755m	2853m	2885m	2894m	2676m	2696m	2738m	2906,5m
Run	2B	2B	2C	2C	2B	2B	2C	2C	2C	2B	2C	2B	2B
Grain-size	med	med-coa	fine-med	upper fine	lower fine	upper fine	med-v.coa	med-coa	fine	lower med	lower fine	lower fine	lower fine
Sorting	moderat	moderat	well	moderat	very well	moderat	very poor	very poor	well	well	well	well	well
Detrital quartz, total	33,67	41,00	33,00	37,00	18,33	27,00	49,67	28,00	26,33	present	present	present	present
Detrital quartz, mono	28,67	35,33	28,00	31,67	17,00	18,33	29,00	21,33	20,00	present	present	present	present
Detrital quartz, poly	5,00	5,67	5,00	5,33	1,33	8,67	20,67	6,67	6,33	present	present	present	present
Detrital feldspar, total	16,33	11,00	13,67	12,33	16,67	18,00	15,67	16,67	15,00	present	present	present	present
Detrital plagioclase	13,33	7,30	10,67	10,00	12,33	14,67	12,67	11,67	13,67	present	present	present	present
Undissolved plagioclase	6,00	1,67	5,33	4,67	3,67	7,67	4,33	3,33	7,00	present	present	present	present
Dissolved plagioclase	7,33	5,67	5,33	5,33	8,67	7,00	8,33	8,33	6,67	present	present	present	present
Detrital kalifeldspar	3,00	4,00	3,00	2,33	4,33	3,33	3,33	5,00	1,33	present	present	present	present
Undissolved kalifeldspar	2,67	3,33	2,00	2,00	3,00	2,33	3,00	2,00	1,00	present	present	present	present
Dissolved kalifeldspar	0,33	0,67	1,00	0,33	1,33	1,00	0,33	3,00	0,33	present	present	present	present
Rock fragments	2,00	7,30	1,70	4,30	2,00	3,70	7,30	6,30	3,30	present	present	present	present
Plutonic	1,67	6,67	1,33	3,33	0,00	3,00	7,33	5,00	0,33				
Metamorphic	0,00	0,00	0,00	0,00	0,00	0,00	0,00	0,67	2,00				
Muscovite	0,00	0,33	0,00	1,00	3,67	2,33	1,00	1,00	2,33	present	present	present	present
Biotite	5,67	3,00	5,33	5,67	26,00	12,00	0,33	4,33	26,67	present	present	present	present
Chert	0,00	0,00	0,00	0,00	0,33	0,33	0,00	0,00	0,00				present
Mud clasts	0,33	0,67	0,33	1,00	1,67	0,33	0,00	0,67	1,00	present			
Fe-Ti mineral	0,33	0,33	1,00	0,33	0,00	0,00	0,00	0,00	0,67	present	present	present	present
Biogenic	0,00	0,00	0,00	0,00	0,00	0,00	0,00	0,00	0,00				
Organic material	3,30	0,30	3,00	3,70	4,70	5,30	1,30	5,30	4,70	present	present	present	present
Glauconite	5,67	6,67	8,00	1,67	trace	0,00	0,33	0,00	0,00	present	present		present
Matrix	0,00	1,00	0,67	5,70	0,00	0,70	7,00	0,00	0,00				
Zircon	trace	trace	trace	trace	0,33	trace	trace	trace	trace	present	present	present	present
Authigene quartz	1,33	2,67	3,33	2,00	4,33	2,67	1,33	3,00	4,33	present	present	present	present
Authigene plagioclase	0,00	0,33	0,00	0,00	0,00	0,00	0,33	0,00	0,00			present	
Authigene clay	15,00	5,33	7,33	9,67	4,67	10,00	5,33	8,67	6,00	present	present	present	present
Chlorite	0,00	0,00	0,00	0,67	0,33	3,67	0,00	2,67	1,00	present	present	present	present
Illite	0,00	0,00	1,33	2,00	0,67	0,67	1,67	0,33	0,00	present	present	present	present
Kaolinite	15,00	5,33	6,00	7,00	3,67	5,67	3,67	5,67	5,00	present	present	present	present
Siderite	0,00	0,00	trace	0,00	0,00	0,00	0,00	9,33	0,00	present	present		
Calcite	0,67	13,00	3,67	2,00	1,33	0,00	0,67	0,33	0,33	present	present	present	present
In pore-space	0,00	11,00	3,33	2,00	1,33	0,00	0,67	0,00	0,00				
Replasive	0,00	2,00	0,33	0,00	0,00	0,00	0,00	0,33	0,33				
Pyrite	0,70	0,33	0,00	5,00	1,00	1,00	1,00	1,30	0,33	present	present	present	present
Ti-oxid	3,00	0,30	4,00	1,70	5,00	4,70	0,70	4,00	5,30	present	present	present	present
Goethite	0,00	0,00	0,00	0,00	1,70	0,00	0,00	0,00	0,00				
K-minerals, total	16,67	21,97	19,70	17,97	38,33	22,37	13,97	17,63	34,63				
Porosity, total	12,33	7,00	15,33	7,67	10,33	12,67	7,67	11,00	4,33				
Porosity, primary	0,67	1,33	1,67	2,00	1,00	0,67	0,33	1,00	0,33				
Porosity, secondary	11,67	5,67	13,67	5,67	9,33	12,00	7,33	10,00	4,00				
In kaolinite	0,33	0,00	0,67	0,67	0,00	0,33	0,33	0,33	0,33				
In plagioclase	7,00	3,00	8,67	2,00	5,33	6,33	4,00	5,33	2,00				
In kalifeldspar	0,33	1,00	0,00	0,00	0,33	1,67	0,00	2,00	0,00				
In calcite	0,00	0,67	0,00	0,00	0,00	0,00	0,00	0,33	0,00				
In mica	0,00	0,33	0,33	0,00	1,33	2,00	0,33	0,33	1,00				
Secondary, undefined	4,00	0,67	4,00	3,00	2,33	1,67	2,67	1,67	0,67				
Quartz	64,33	68,33	66,89	68,52	49,11	55,48	68,04	54,19	58,09				
Feldspar	31,21	18,89	27,70	22,84	44,64	36,99	21,92	32,26	33,09				
Lithic	4,46	12,78	5,41	8,64	6,25	7,53	10,05	13,55	8,82				
"Original" values													
Quartz	44,89	57,48	50,77	58,12	39,29	43,09	61,32	42,86	49,69				
Feldspar	52,00	31,78	45,13	34,55	55,71	51,06	29,63	46,43	42,77				
Lithic	3,11	10,75	4,10	7,33	5,00	5,85	9,05	10,71	7,55				

Table 1. Point counting data in percent from selected thin sections from Qulleq-1, where an amount of 300 points could be obtained.

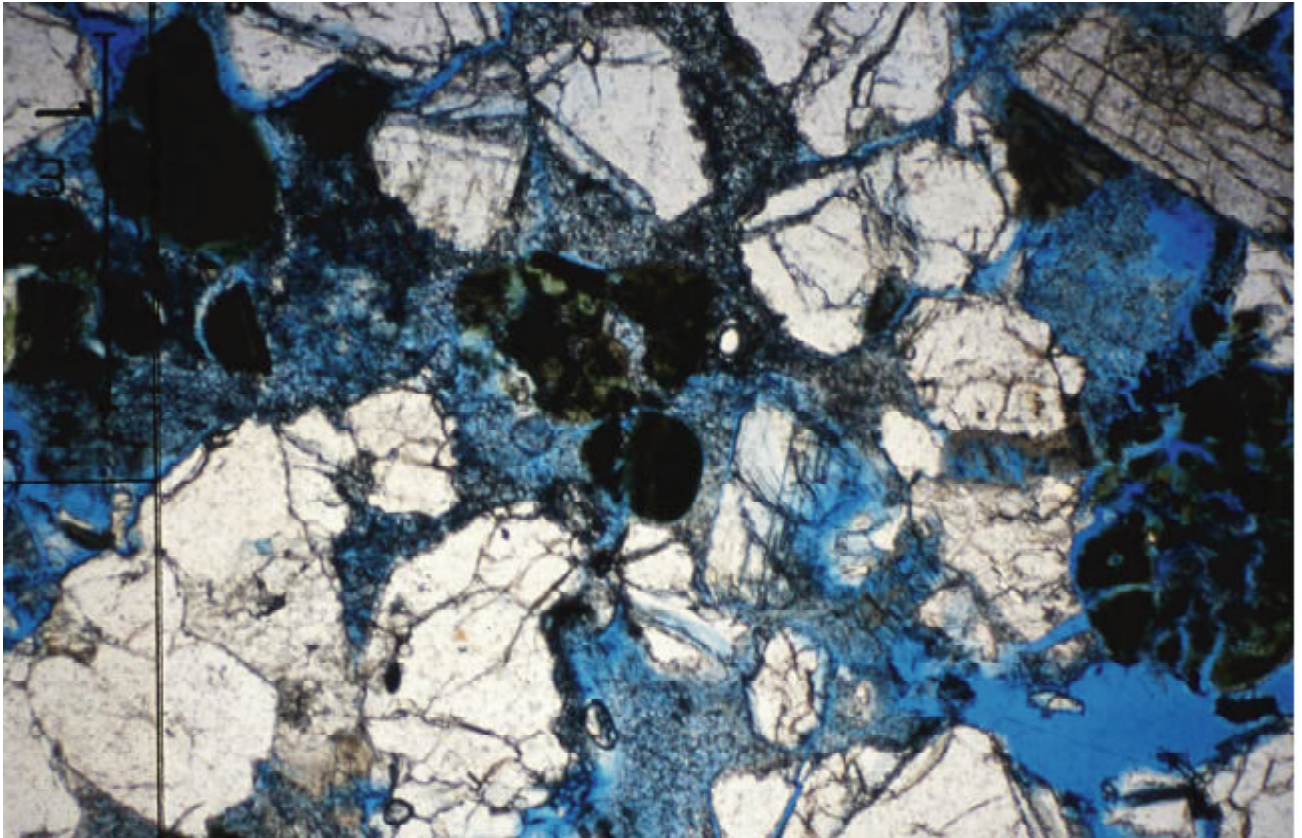


Plate 1: Sample 2662m, PN: See below.

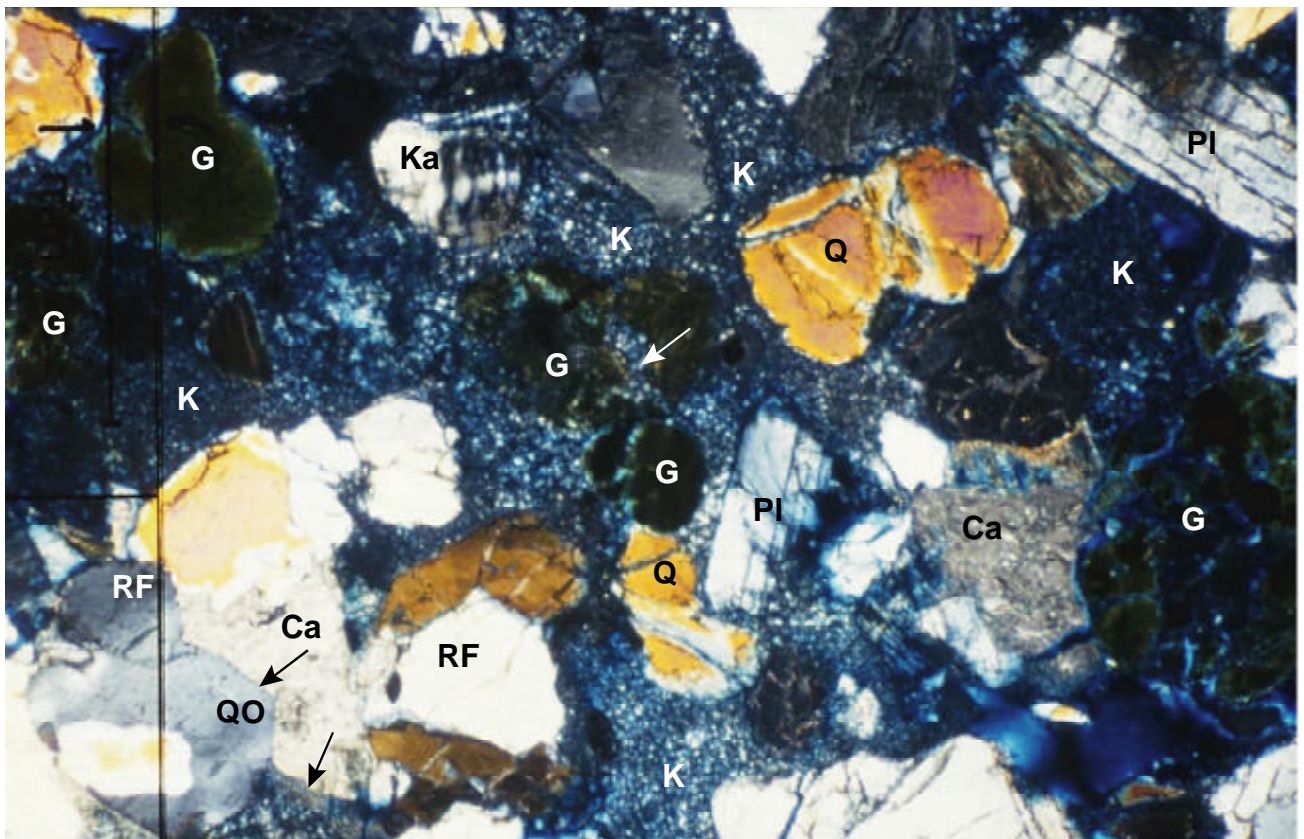


Plate 2: Sample 2662m, XN: Dark green glauconite grains (G) with kaolinite (K) in cracks (white arrow). Kaolinite replaces grains and occurs as intergranular cement. Lower left is a partly dissolved rock fragment (RF), which probably experienced feldspar dissolution followed by quartz overgrowth (QO). Later calcite cementation (Ca) cemented quartz overgrowth (long black arrow) and kaolinite (short black arrow). Kalifeldspar (Ka), plagioclase (PI) and quartz (Q).

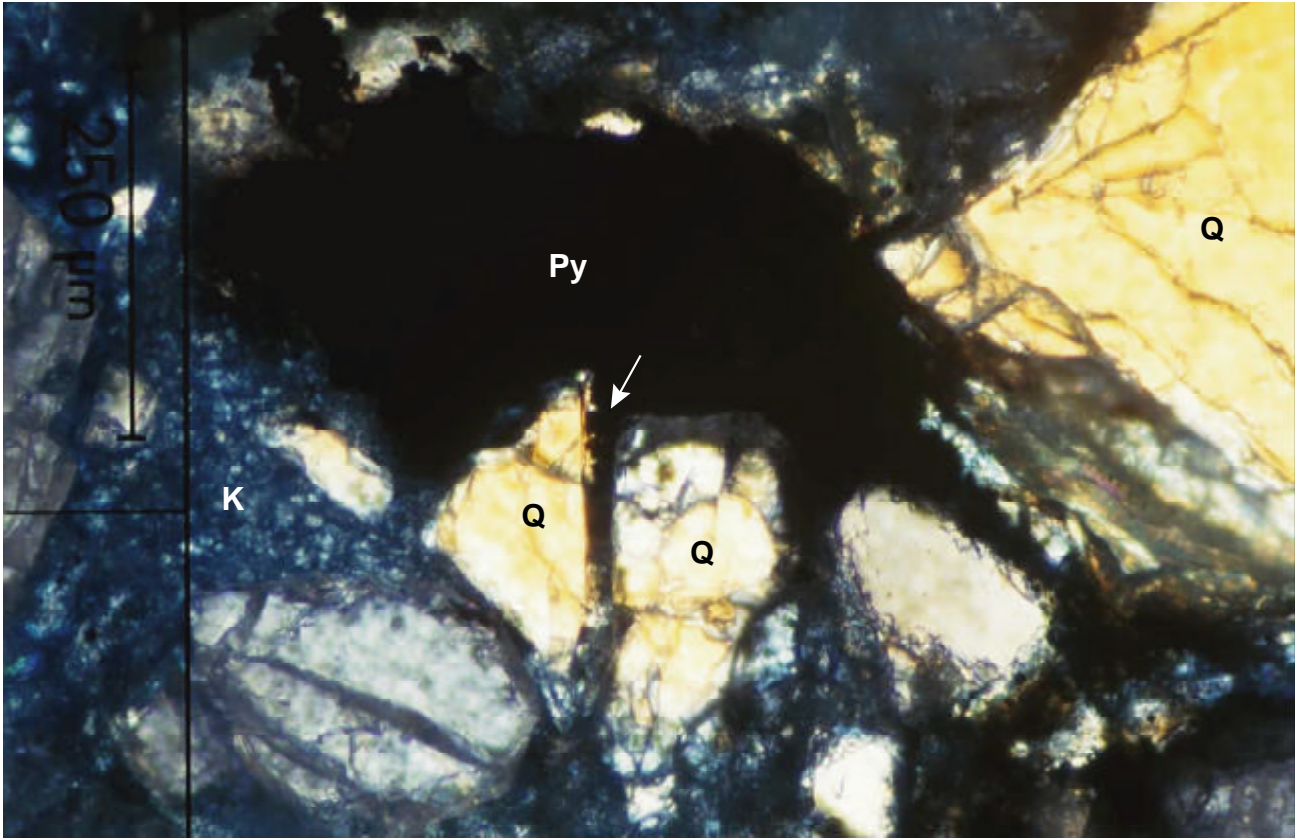


Plate 3: Sample 2682m, XN: Pyrite (Py) precipitation in mechanical crushed quartz grain (white arrow). Kaolinite (K).

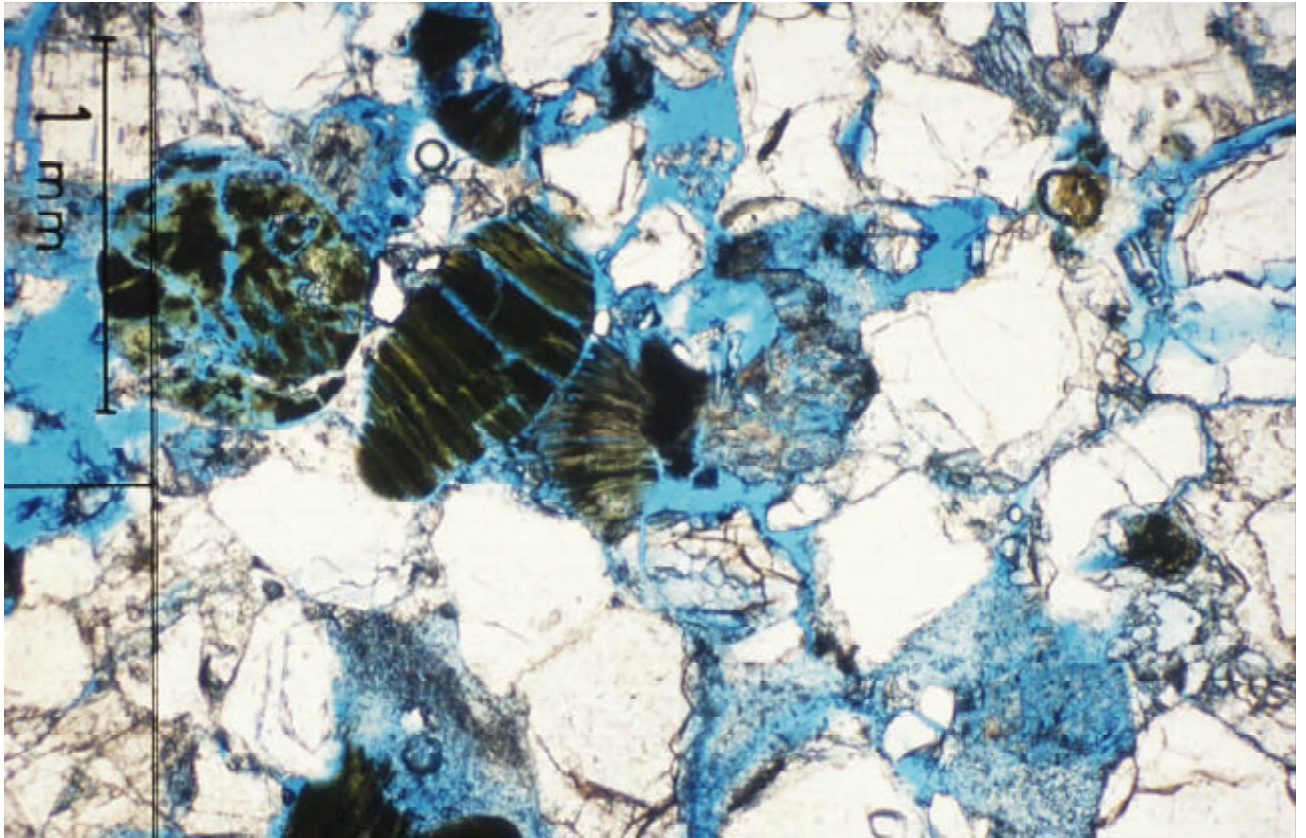


Plate 4: Sample 2662m, PN: See below.

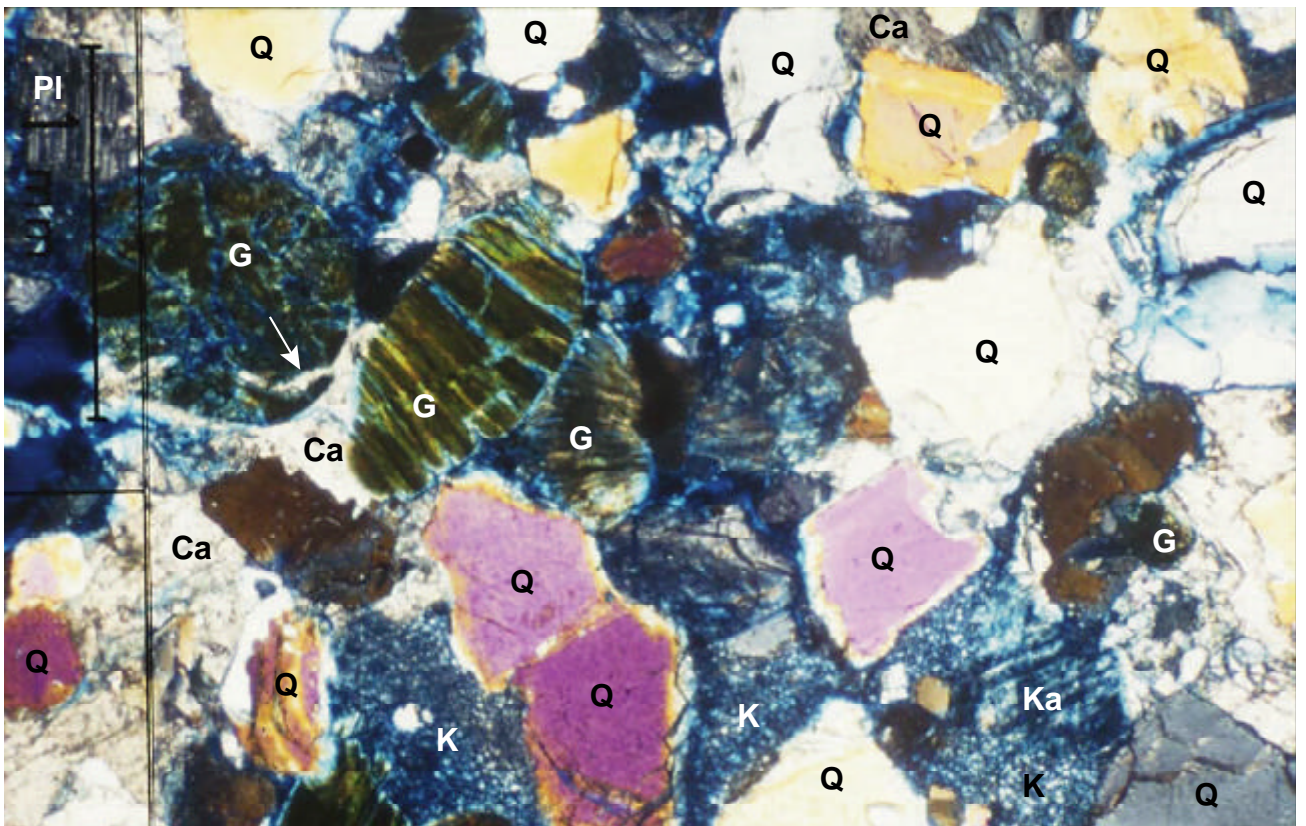


Plate 5: Sample 2662m, XN: Dark green, rounded glauconite grains (G) cemented by calcite (Ca). The glauconite grain to the upper left is cracked with later calcite ingrowths (white arrow). Kaolinite (K) in oversized pore space probably replaces feldspars. Lower right: Dissolved kalifeldspar (Ka) with secondary porosity is surrounded by kaolinite, which post dates feldspar dissolution. Quartz (Q) and plagioclase (Pl).

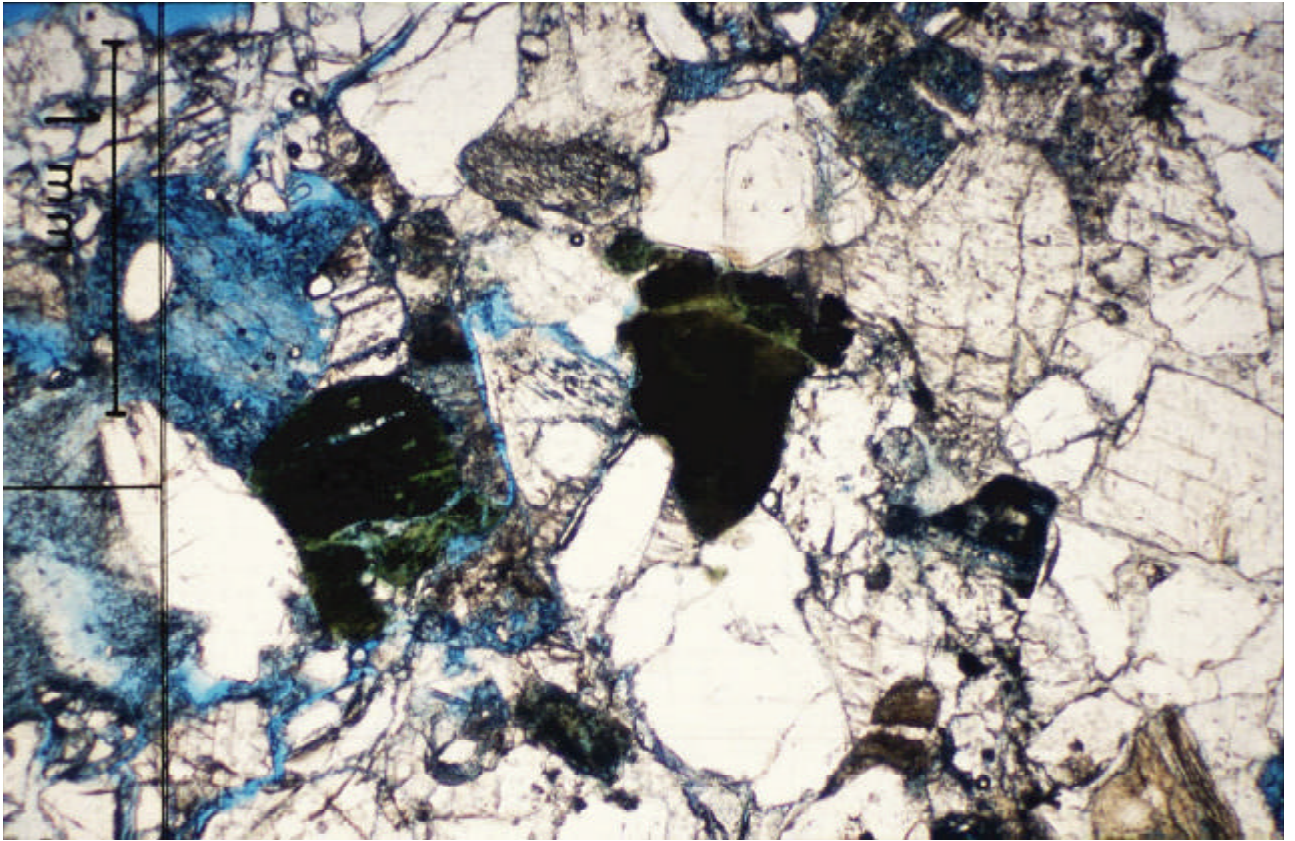


Plate 6: Sample 2662m, PN: See below.

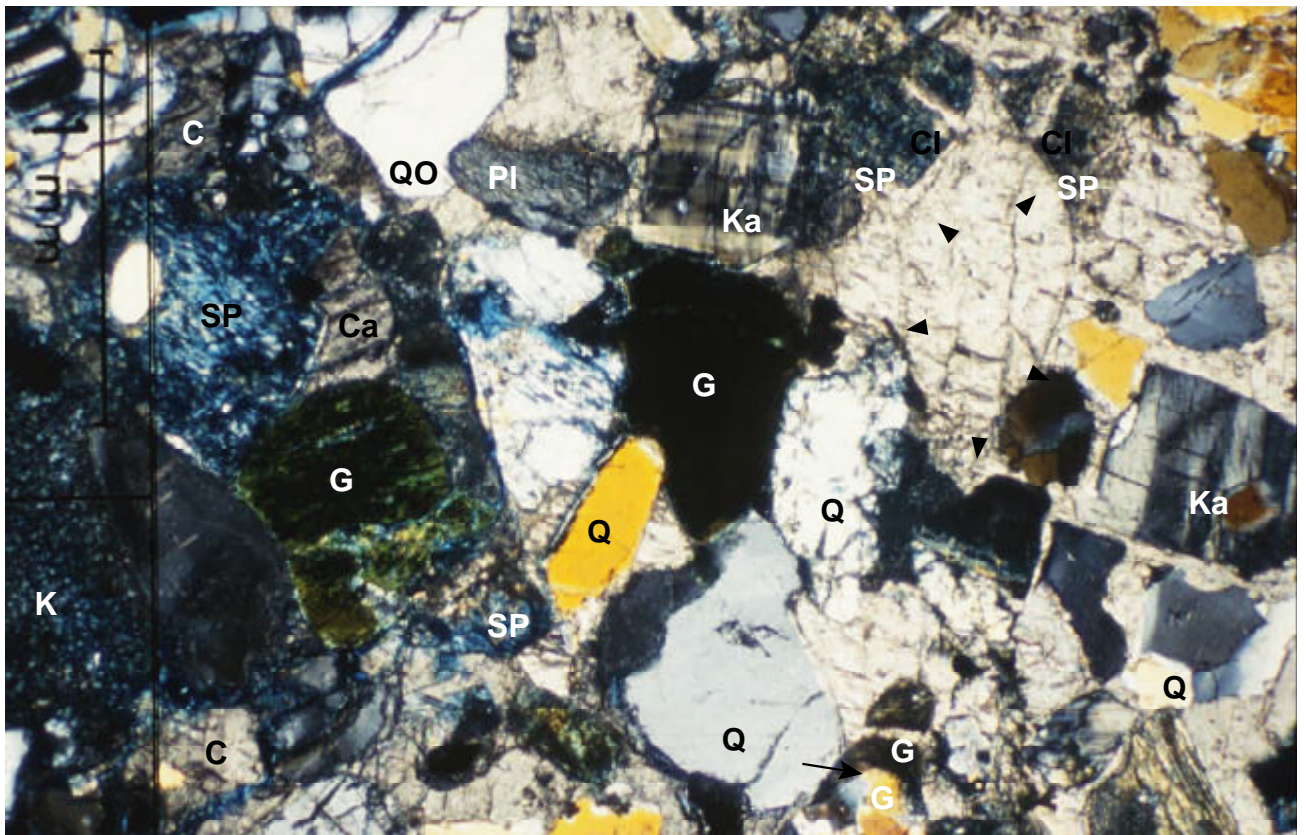


Plate 7: Sample 2662m, XN: Dark green, glaucanite grains (G), the one in the centre is deformed due to compaction and one at the bottom is cracked and later healed by calcite (black arrow). Feldspar grain to the far left is replaced by kaolinite (K). Calcite cement surrounds secondary porosity (SP) due to later feldspar grain dissolution and calcite ingrowths in feldspar cracks (CI) stand back after grain dissolution. Plagioclase grain (PI) right to the upper centre has been partly cemented by earlier quartz overgrowth (QO) before calcite cementation. The outline of a calcite-replaced grain is indicated by small, black triangles. Quartz (Q) and rock fragments grains.

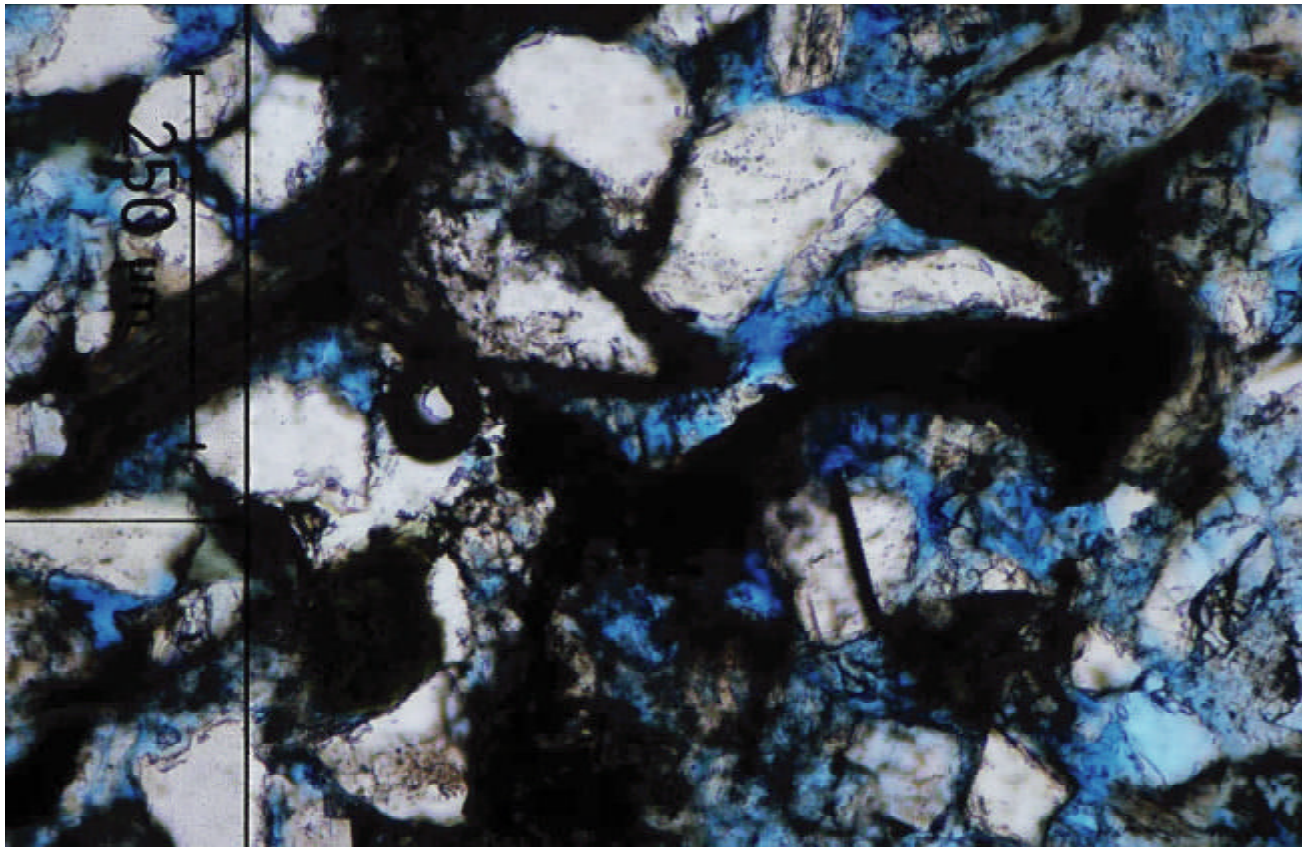


Plate 8: Sample 2686m, PN: See below.

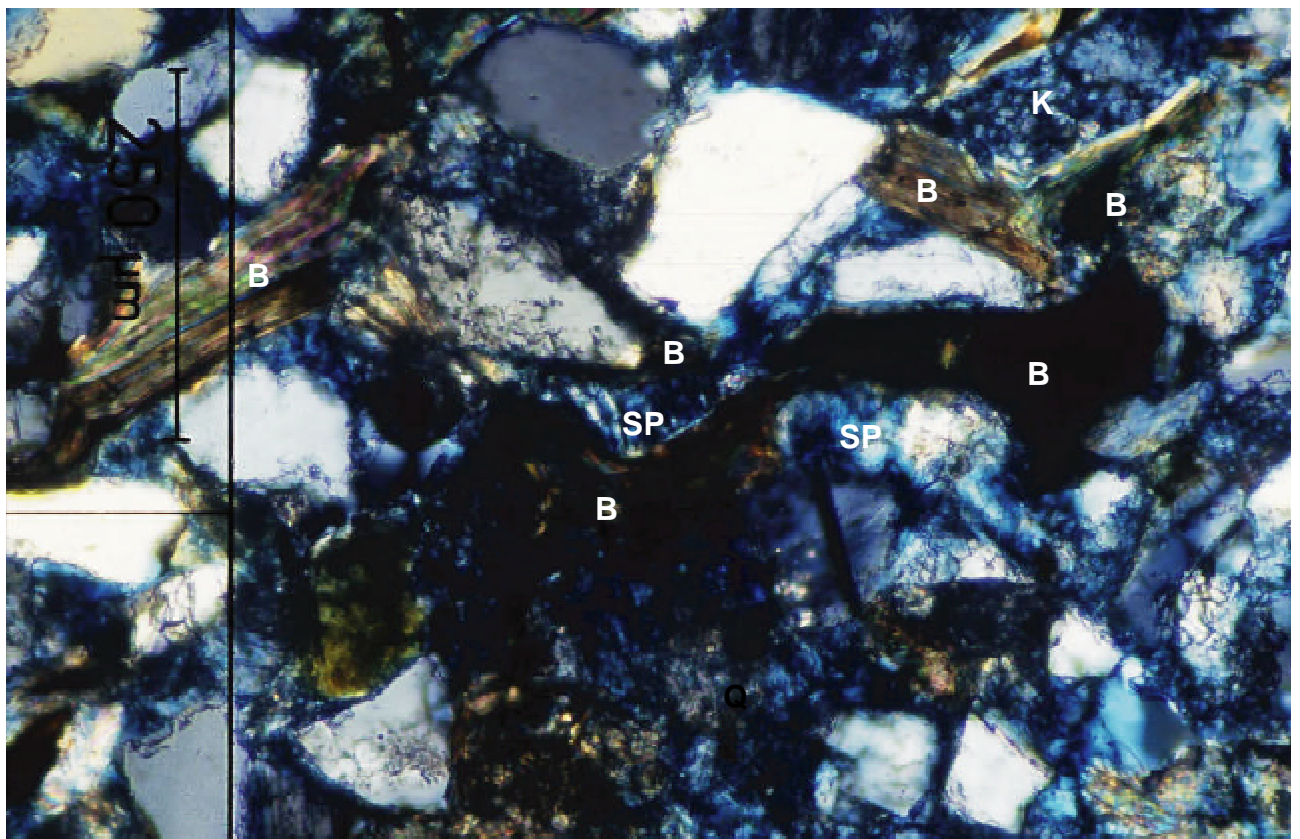


Plate 9: Sample 2686m, XN: Biotite grains (B) are mechanical compacted around kaolinite-replaced (K) and dissolved feldspar grains revealing secondary porosity (SP). This indicates that replacement and dissolution post-date mechanical compaction.

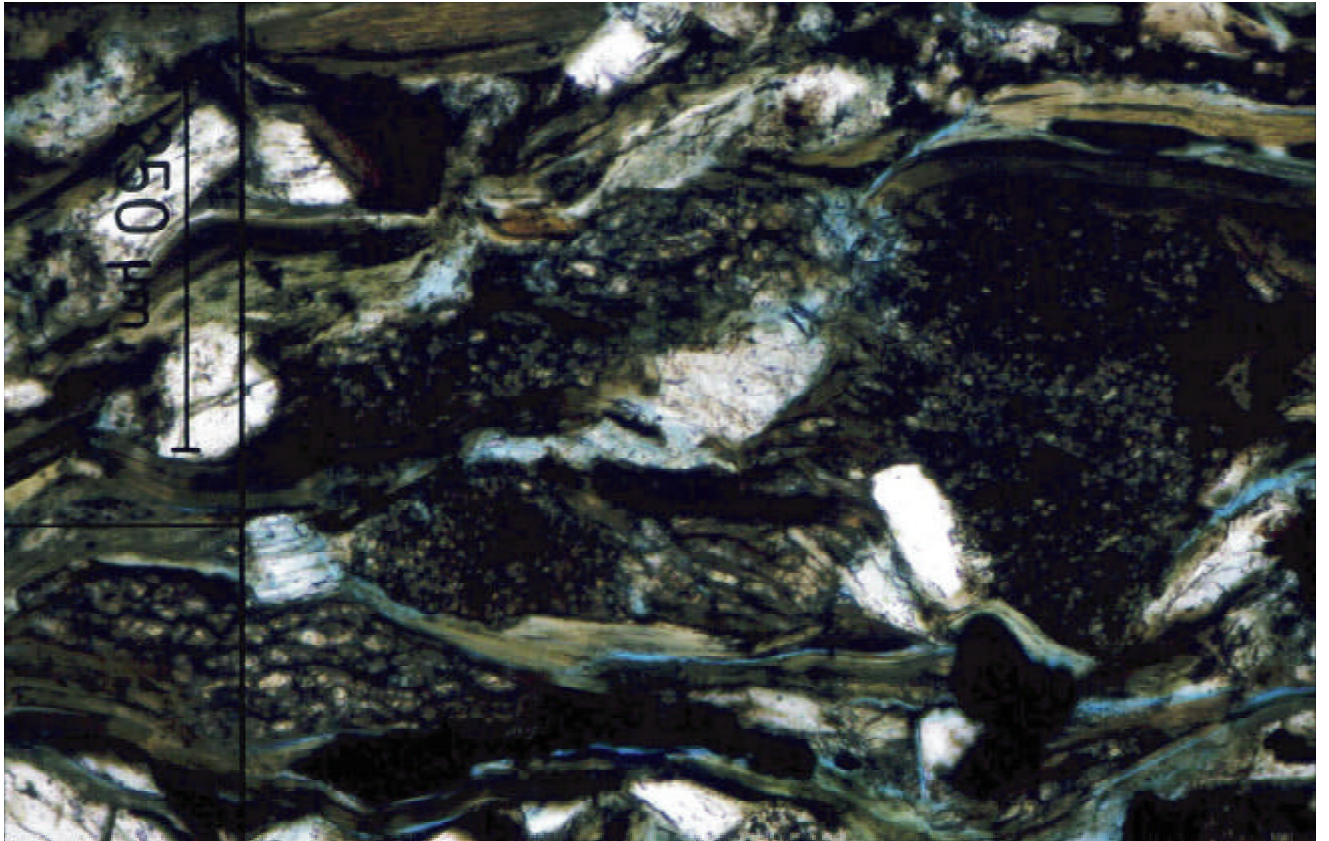


Plate 10: Sample 2686m, PN: See below.

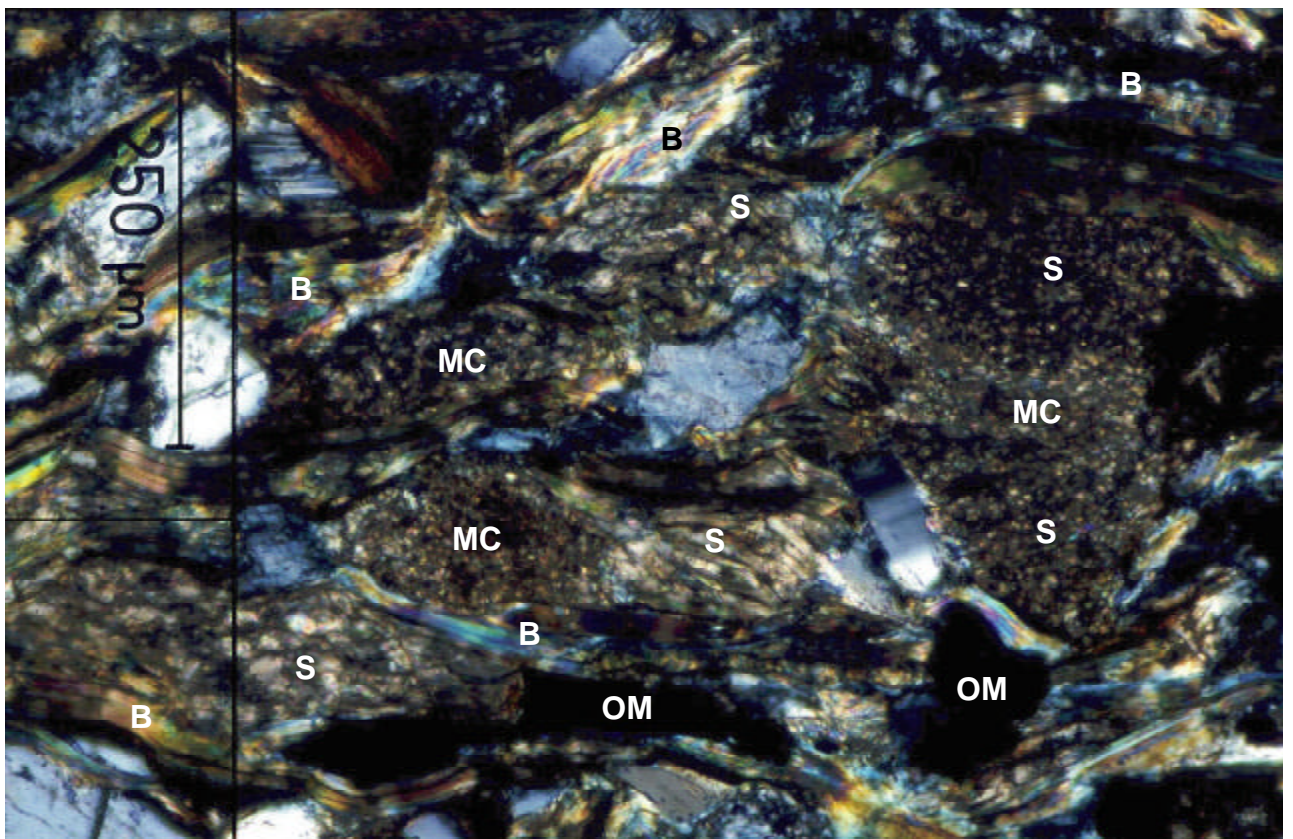


Plate 11: Sample 2686m, XN: Siderite rhombs (S) precipitated along cleavage plans in biotite (B) and in mud clasts (MC). Organic material (OM).

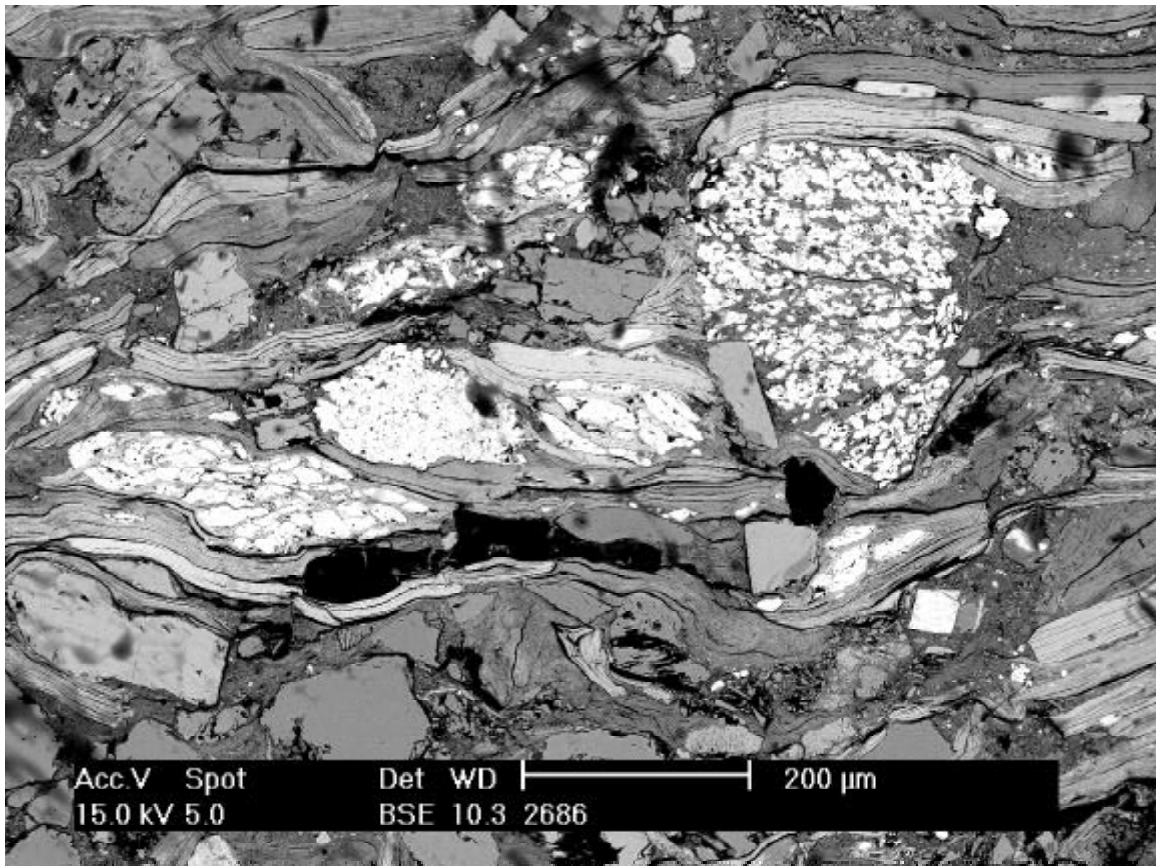


Plate 12: Sample 2686m, SEM-Backscatter: The same picture as plate 10 and 11. The high density of the siderite crystals gives them a bright appearance, as well as density variation in the biotite grains can be observed. The precipitation of siderite follows the mechanical deformed biotite grains thus post dating compaction. Organic material is black

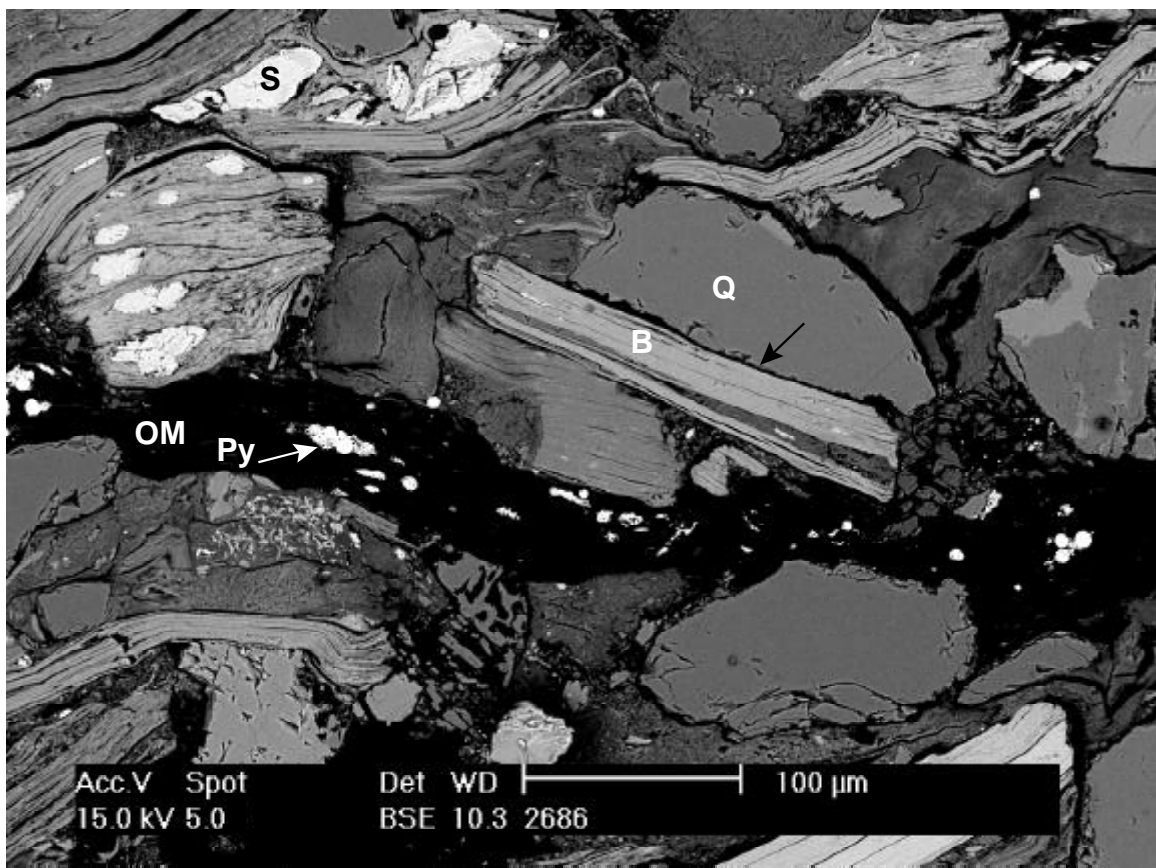


Plate 13: Sample 2686m, SEM-Backscatter: Black organic material (OM) with bright pyrite (Py) precipitation. Upper left are seen bright siderite rhombs (S) precipitated along cleavage plans in compacted biotite. Pressure dissolution is indicated by the tangential contact (black arrow) between quartz (Q) and biotite (B) grain.

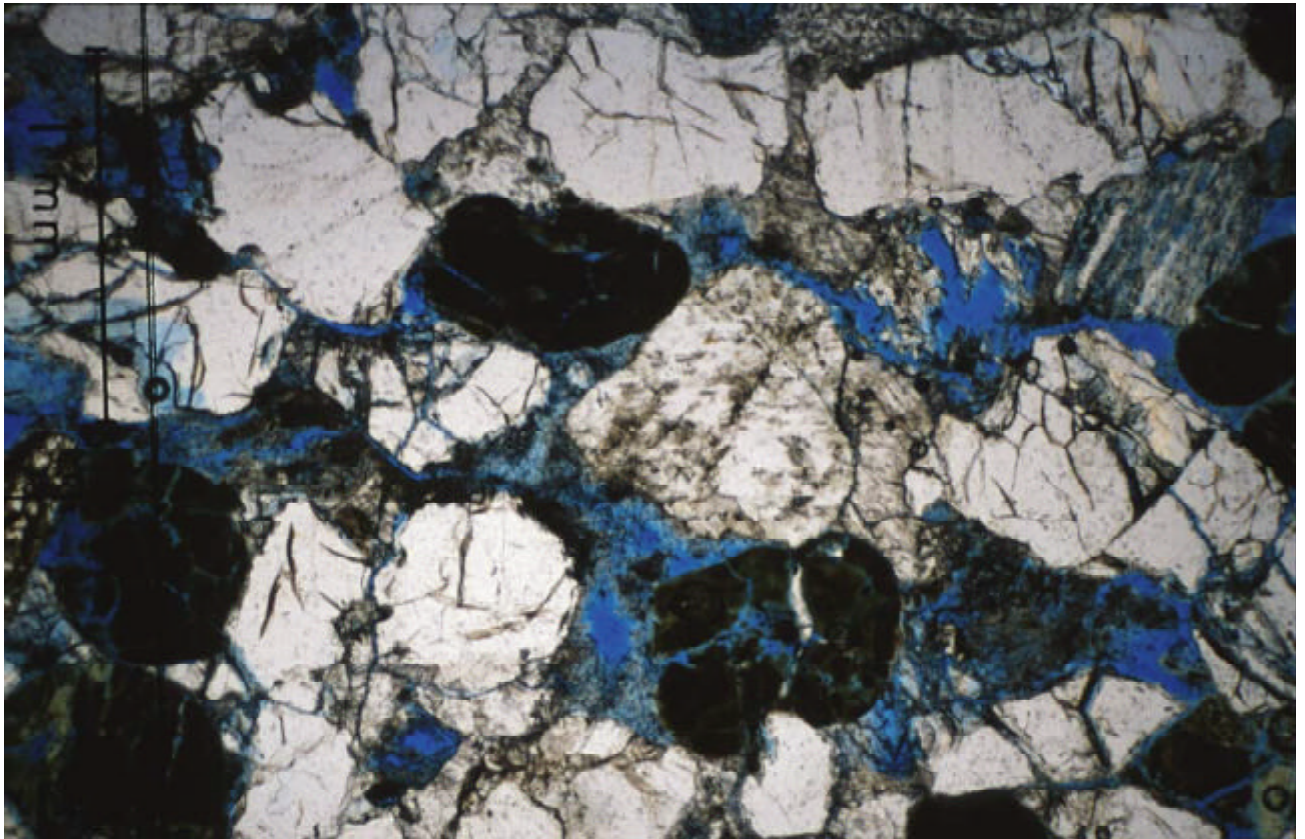


Plate 14: Sample 2662m, PN: See below.

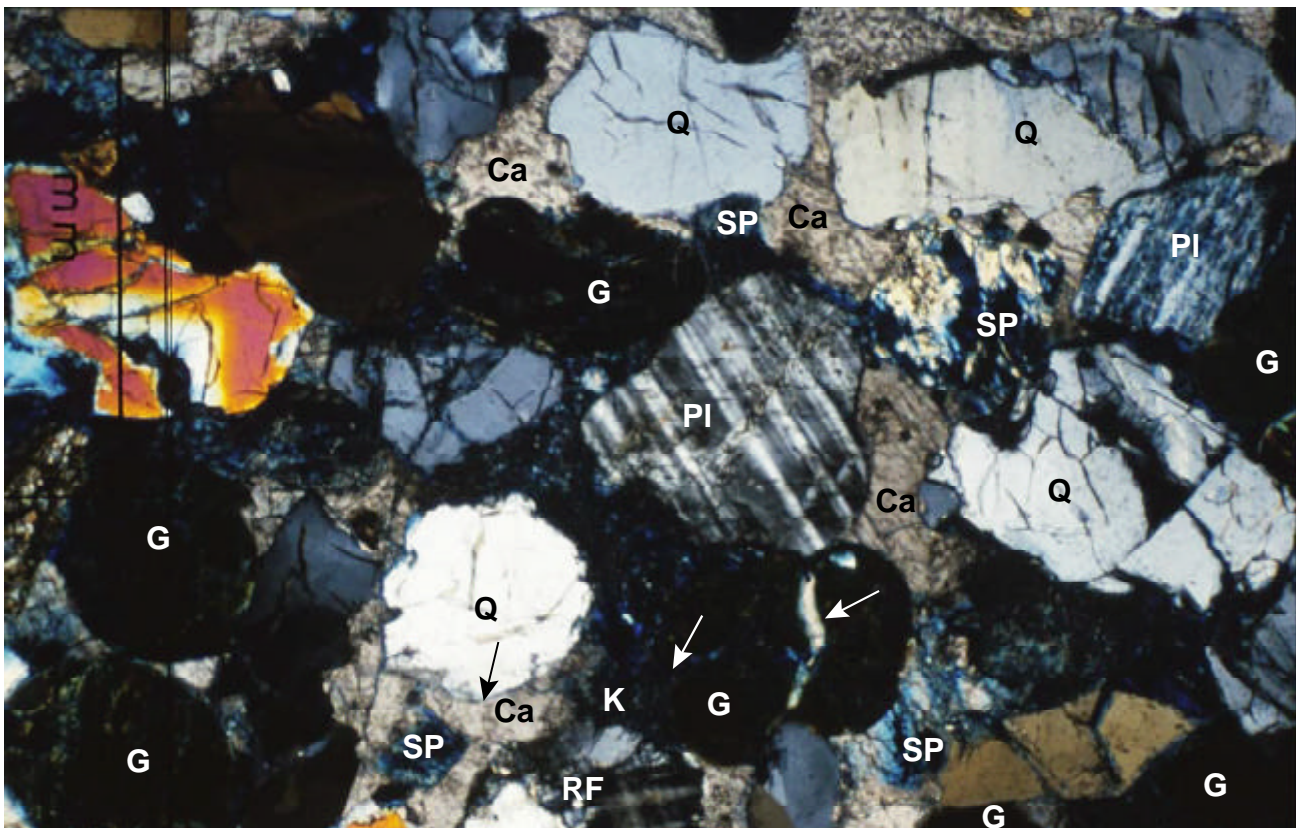


Plate 15: Sample 2662m, XN: Dark green, rounded glauconite grains (G) cracked at grain contacts. The compaction cracks (white arrows) are partly filled with kaolinite (K) and calcite (Ca). Calcite also forms patchy intergranular cement revealing secondary porosity (SP) after later feldspar dissolution. Calcite cements quartz overgrowth (black arrow). Quartz grains (Q) and rock fragment (RF).

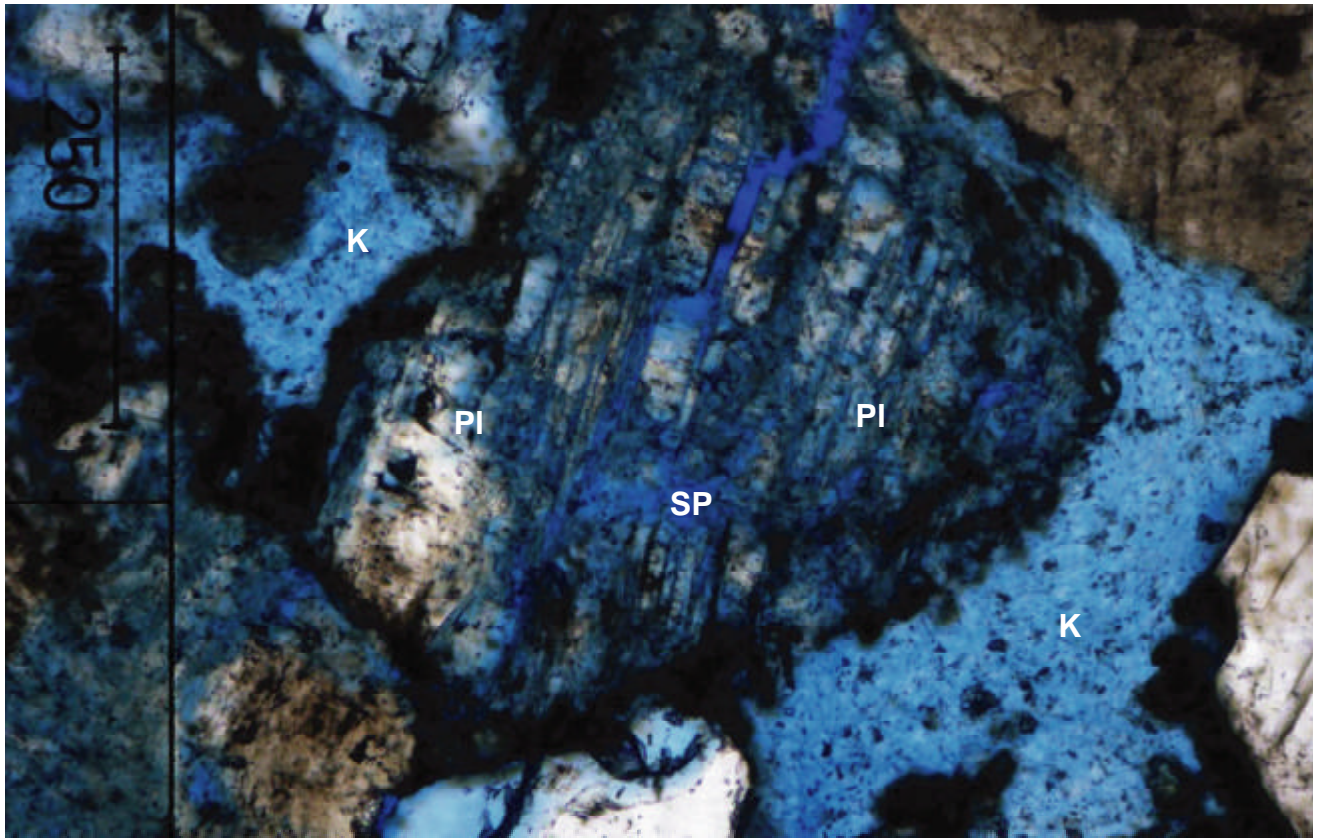


Plate 16: Sample 2885m, PN: Partly dissolved plagioclase grain (PI) with intragranular, secondary porosity (SP) surrounded by early kaolinite (K).

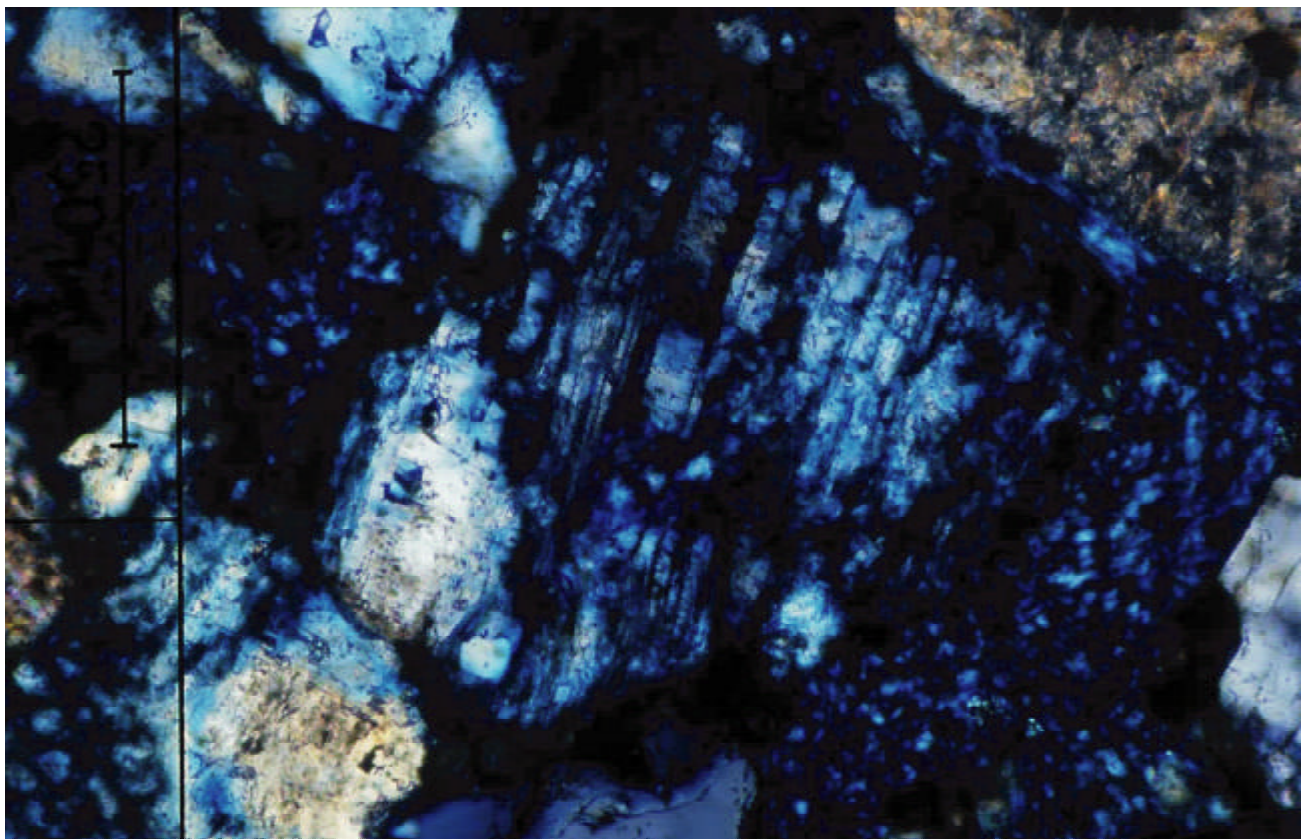


Plate 17: Sample 2885m, XN: See above.

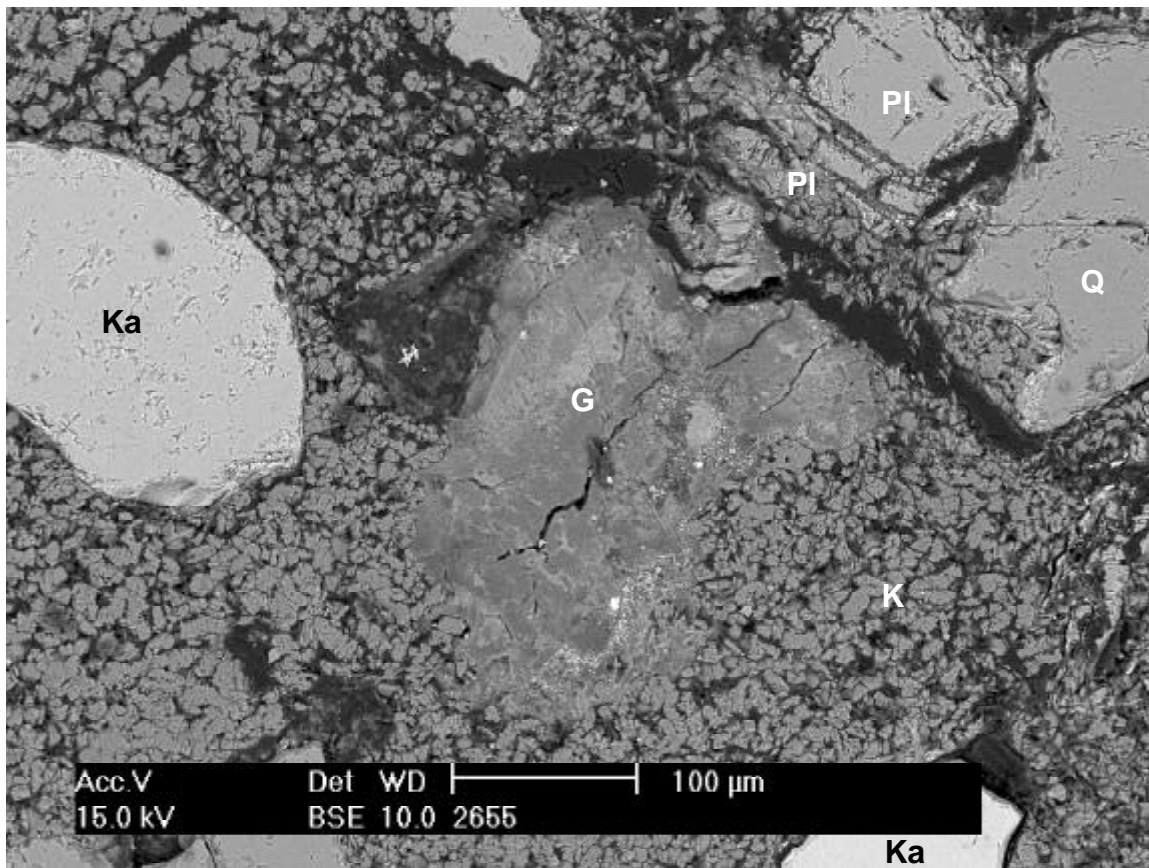


Plate 18: Sample 2655m, SEM-Backscatter: Glauconite (G), quartz (Q), plagioclase (PI) and rounded kalifeldspar grains (Ka) are surrounded by kaolinite booklets (K) precipitated in intergranular and oversized pore space.

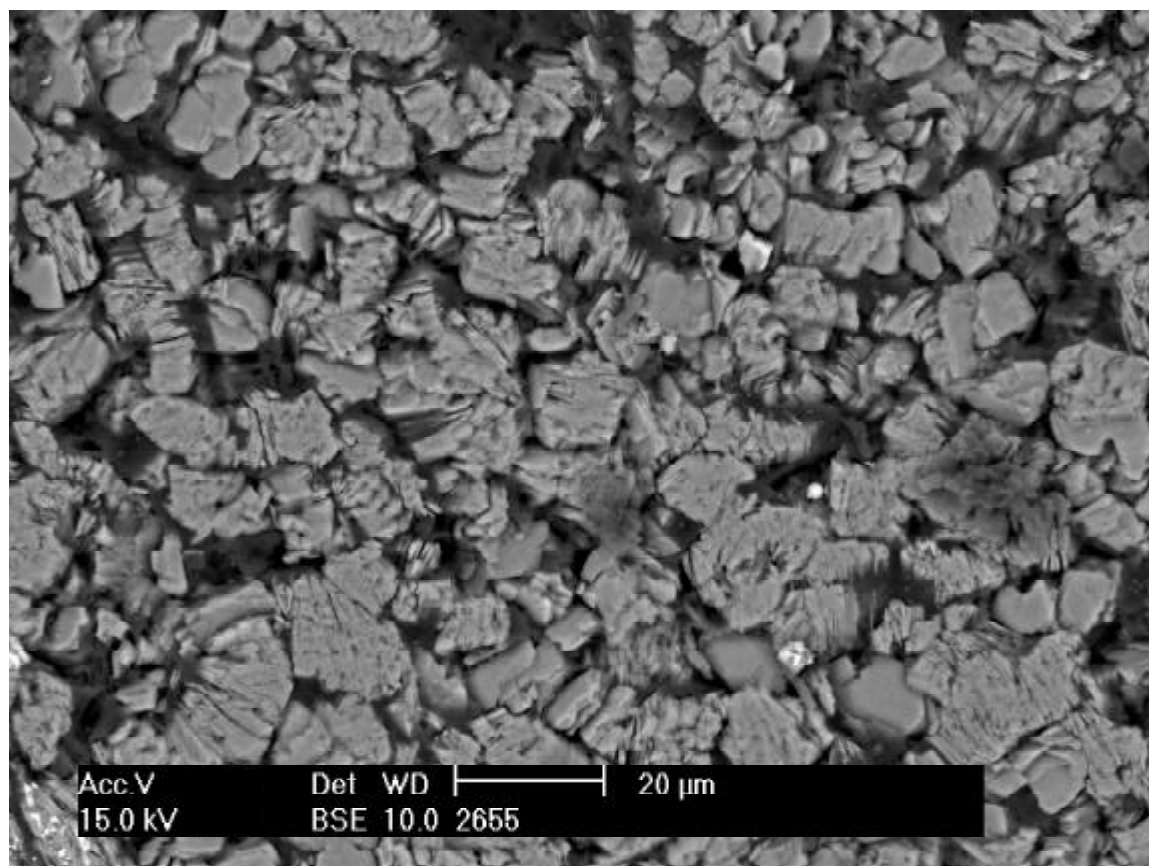


Plate 19: Sample 2655m, SEM-Backscatter: Kaolinite booklets with intergranular microporosity.

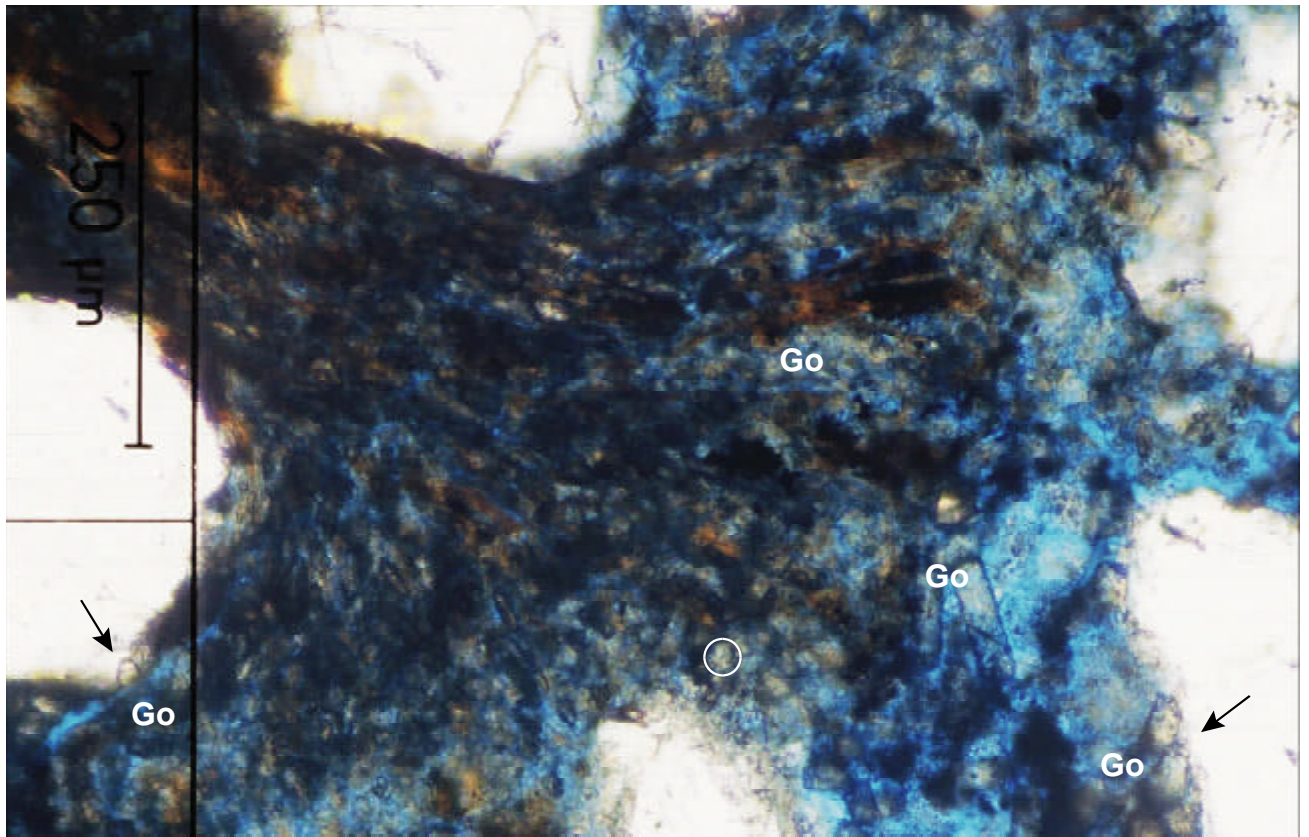


Plate 20: Sample 2885m, XN: Goethite crystals (Go) are precipitated in and near a compacted and intensively degraded biotite grain. Some of the goethite crystals reveal a hexagonal form in transverse section (encircled). Some of the goethite crystals are overgrown by quartz (black arrows).

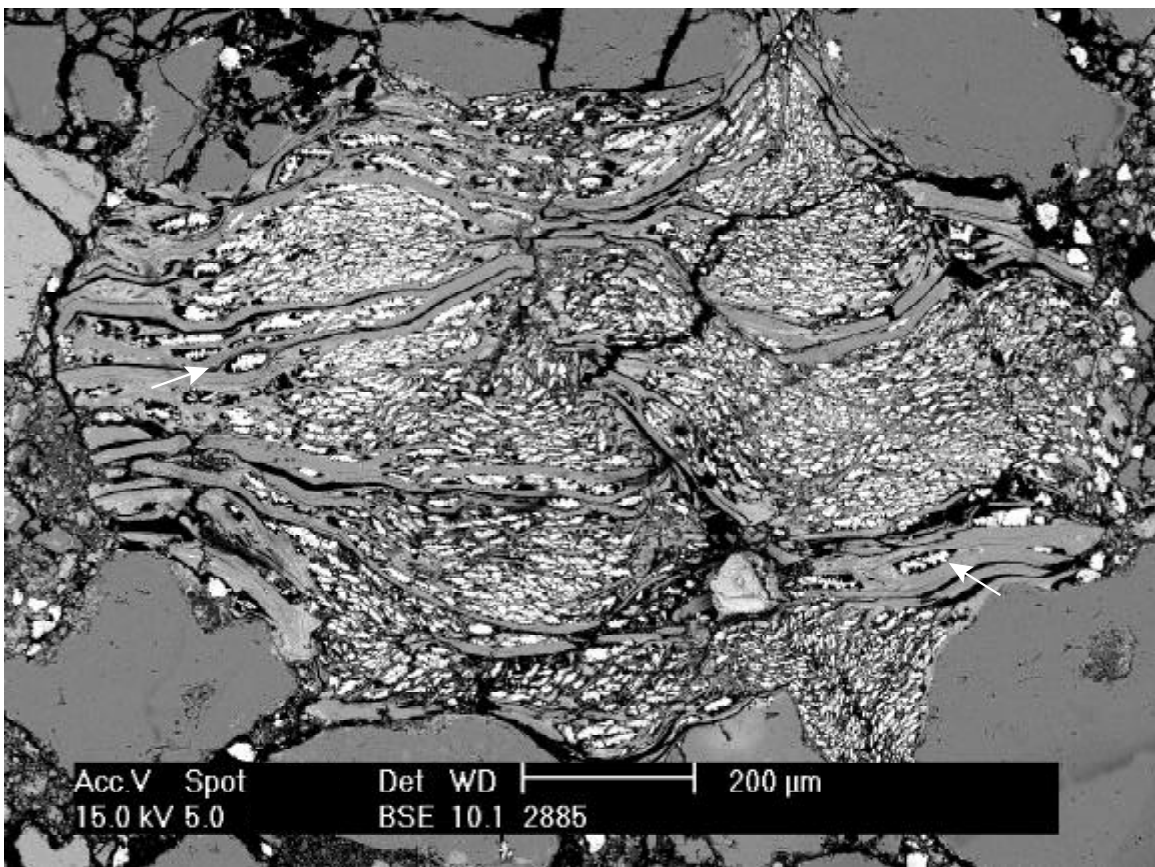


Plate 21: Sample 2885m, SEM-Backscatter: Bright, goethite crystals have replaced siderite rhombs in expanded biotite grain. Partly dissolved goethite crystals reveal the rhombic morphology of the replaced siderite crystals (white arrows) Larger goethite crystals are seen in the pore space to the right.

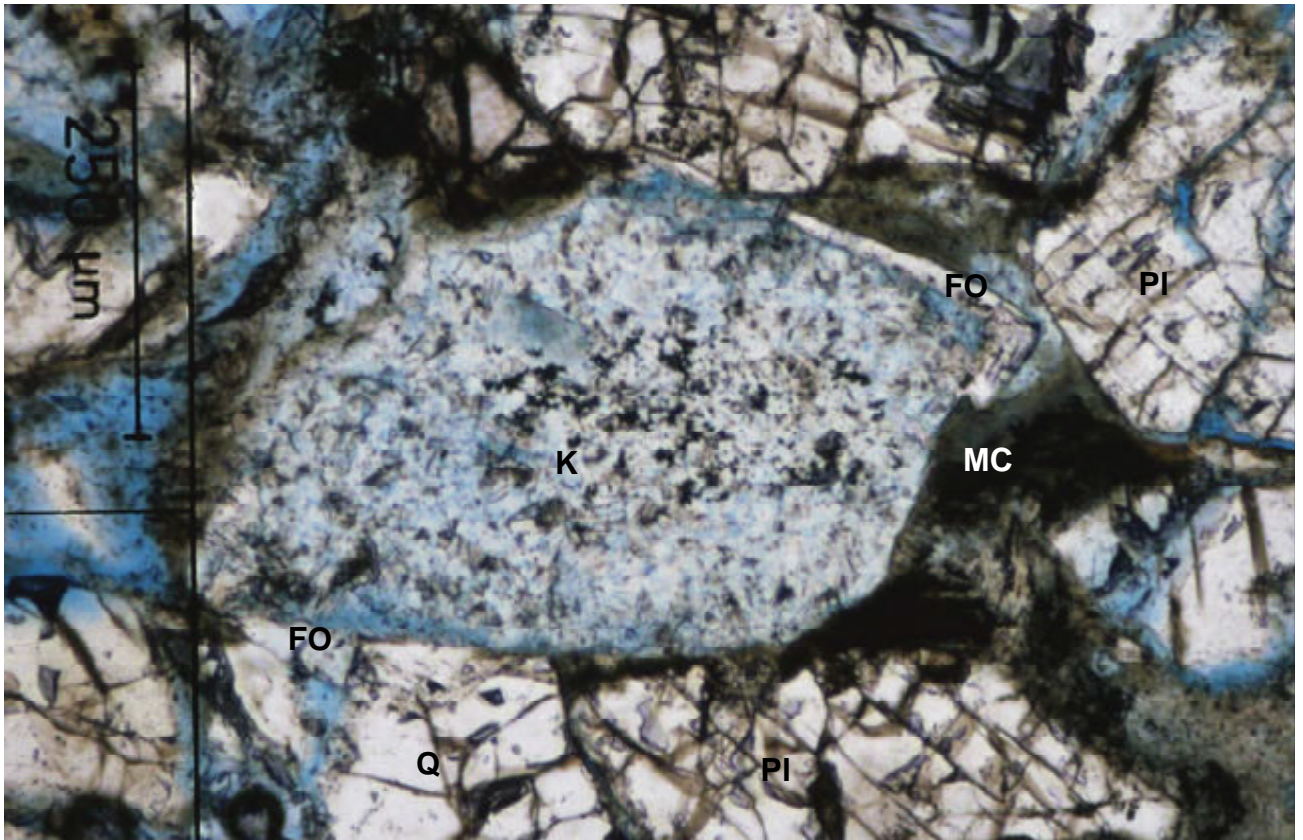


Plate 22: Sample 2894m, PN: Feldspar overgrowths (FO) on kaolinite (K) replaced grain. The overgrowths are restricted by a compacted mudstone clast (MC) to the right and a quartz grain (Q) to the lower left. Detrital plagioclase (PI) and quartz grains (Q).

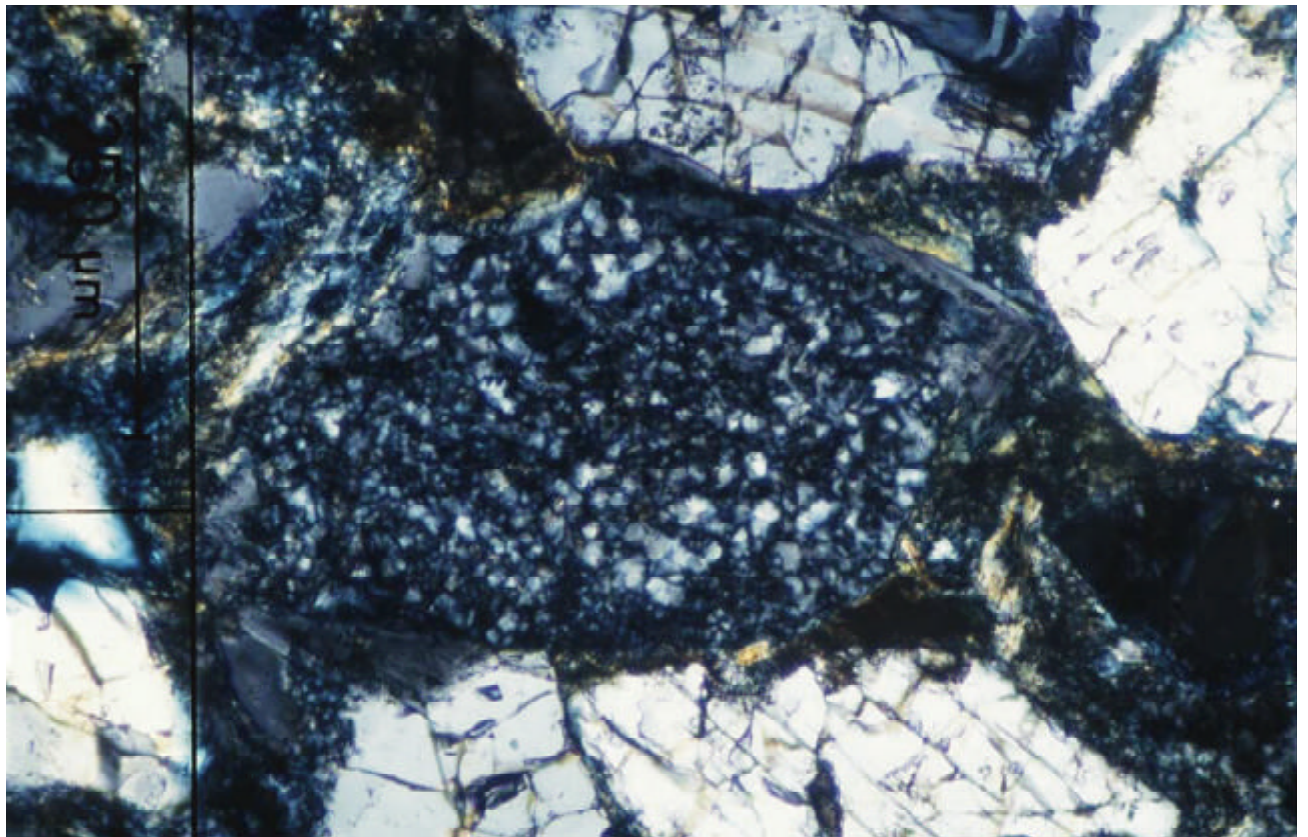


Plate 23: Sample 2894m, XN: See above

*Danmarks og Grønlands Geologiske Undersøgelse  
(GEUS) er et forsknings- og rådgivningsinstitut i  
Miljø- og Energiministeriet*

Danmarks og Grønlands  
Geologiske Undersøgelse (GEUS)  
*Geological Survey of Denmark and Greenland*

Thoravej 8  
2400 København NV  
Danmark

Telefon 38 14 20 00  
Fax 38 14 20 50  
E-post [geus@geus.dk](mailto:geus@geus.dk)  
Hjemmeside [www.geus.dk](http://www.geus.dk)